Atmospheric Pollution Research 3 (2012) 55-71

Atmospheric Pollution Research

www.atmospolres.com

Simulation of surface ozone pollution in the Central Gulf Coast region during summer synoptic condition using WRF/Chem air quality model

Anjaneyulu Yerramilli, Venkata Srinivas Challa, Venkata Bhaskar Rao Dodla, LaToya Myles, William R. Pendergrass, Christoph A. Vogel, Francis Tuluri, Julius M. Baham, Robert Hughes, Chuck Patrick, John Young, Shelton Swanier

Trent Lott Geospatial and Visualization Research Centre @Mississippi e–Centre, Jackson, Jackson State University, MS 39217, USA

ABSTRACT

WRF/Chem, a fully coupled meteorology–chemistry model, was used for the simulation of surface ozone pollution over the Central Gulf Coast region in Southeast United States of America (USA). Two ozone episodes during June 8–11, 2006 and July 18–22, 2006 characterized with hourly mixing ratios of 60–100 ppbv, were selected for the study. Suite of sensitivity experiments were conducted with three different planetary boundary layer (PBL) schemes and three land surface models (LSM). The results indicate that Yonsei–University (YSU) PBL scheme in combination with NOAH and SOIL LSMs produce better simulations of both the meteorological and chemical species than others. YSU PBL scheme in combination with NOAH LSM had slightly better simulation than with SOIL scheme. Spatial comparison with observations showed that YSUNOAH experiment well simulated the diurnal mean ozone mixing ratio, timing of diurnal cycle as well as range in ozone mixing ratio at most monitoring stations with an overall correlation of 0.726, bias of –1.55 ppbv, mean absolute error of 8.11 ppbv and root mean square error of 14.5 ppbv; and with an underestimation of 7 ppbv in the daytime peak ozone and about 8% in the daily average ozone. Model produced 1–hr, and 8–hr average ozone values were well correlated with corresponding observed means. The minor underestimation of daytime ozone is attributed to the slight underestimation of air temperature which tend to slow–down the ozone production and overestimation of wind speeds which transport the produced ozone at a faster rate. Simulated mean horizontal and vertical flow patterns suggest the role of the horizontal transport and the PBL diffusion in the development of high ozone during the episode. Overall, the model is found to perform reasonably well to simulate the ozone and other precursor pollutants with good correlations and low error metrics. Thus the study demonstrates the potential of WRF/Chem model for air quality prediction in coastal environments.

Keywords:
Air quality
WRF/Chem
Ozone
Meteorology

Article History:
Received: 28 March 2011
Revised: 31 August 2011
Accepted: 08 September 2011

Corresponding Author:
Anjaneyulu Yerramilli
Tel: +1-601-979-3654
Fax: +1-601-979-8247
E-mail: yerramilli.anjaneyulu@jsums.edu

doi: 10.5094/APR.2012.005

1. Introduction

The Central Gulf Coast region covering Mississippi, Alabama and Louisiana in the Southeast US is environmentally sensitive due to presence of large number of sensitive ecosystems which are of national importance and presently facing threat from multiple air pollution problems originating as a consequence of several developmental activities such as oil and gas refineries, operational thermal power plants and mobile–source pollution. Summer ozone, one of the six criteria pollutants of major significance as per USEPA (United States Environmental Protection Agency), is mainly formed by the oxidation process of volatile organic compounds (VOCs) in the presence of nitrogen oxides NO_x (NO and NO_2) and sunlight intensity. Studies over different regions clearly indicate that the ozone formation is strongly dependent on locations due to the varied ambient chemical conditions in different regions, prevailing meso– and micro–meteorological conditions and the resulting wind flow and turbulence fields (Kleinman et al., 2000; Thielmann et al., 2002; Kleinman et al., 2003; Zaveri et al., 2003). The Central Gulf Coast has large forest and vegetation areas which contribute to high biogenic VOC emissions. Several anthropogenic sources like thermal power plants, oil refineries, manufacturing, metallurgical, paper industries, automobile emissions contribute to photochemical pollution in the region. Ozone episodes in the Central Gulf Coast occur under a variety of regional–scale atmospheric conditions and prevailing circulations. High pressure systems over the mid–south associated with northerly to north–easterly winds, or high pressure over the Gulf of Mexico associated with westerly winds are attributed to influence the development of favorable meteorological conditions for local ozone generation (Douglas et al., 2005). Another cause for the high ozone mixing ratios in the coastal areas of Central Gulf Coast is the recirculation of pollutants by the onshore and offshore flows resulting from the mesoscale wind system called "Gulf breeze" (Douglas et al., 2005). A few studies on air quality from this region (Yerramilli et al., 2008; Challa et al., 2008; Challa et al., 2009) were focused on observational and modeling aspects of the coastal circulation and the plume dispersion from point sources under such mesoscale flow systems.

The development and occurrence of photochemical pollution episodes have been studied using air quality models (AQM) as they incorporate the contributing atmospheric physical and chemical processes (Byun and Ching., 1999; Sistla et al., 2001; Jimenez et al., 2006; Mao et al., 2006; Zhang et al., 2006; Otte et al., 2008). The fully coupled weather–chemistry model – WRF/Chem – (Grell et al., 2005) is the next generation model currently used by many researchers for air quality studies (Zhang et al., 2005; Fast et al., 2006; Misenis et al., 2006; Jiang et al., 2008; de Foy et al., 2008) over different regions. Misenis et al. (2006) used WRF/Chem to study the air quality of the Houston–Galveston area and reported that the model planetary boundary layer (PBL) and land surface model (LSM) schemes affected the simulation of chemical species. Their study indicated that Yonsei University non–local diffusion PBL scheme has given better results for meteorological variables while Mellor–Yamada–Janjic PBL scheme for the ozone predictions. Jiang et al. (2008) studied a continuous photochemical pollution episode in Hong Kong using WRF/Chem to examine the meteorological processes contributing to the formation of high ozone and reported that the northerly air stream associated with high temperatures, stable boundary layer and clear sky conditions favored the high ozone formation in Hong Kong city. De Foy et al. (2008) evaluated the WRF model for the complex wind flows in the Mexico City basin area with data from field campaigns using statistical techniques, cluster analysis of flow trajectories and concentration measurements. Their study for ozone showed the influence of the local and regional scale circulations and their modulation by the synoptic–scale flow patterns to govern the short–range transport in the Mexico City region. Tie et al. (2009) studied the performance of the WRF/Chem for the simulation of ozone and its precursors in Mexico City region using in–situ aircraft measurements of chemical species. They reported that the model was able to capture the timing and location of the ozone concentrations, their association with city plumes and that the model underestimated the ozone mixing ratios by about 0–25%. Zhang et al. (2009) studied the air quality over Mexico City using WRF/Chem and reported that the model performs much better during daytime than nighttime for both chemical species and meteorological variables and different combinations of the available PBL and land surface schemes did not reduce the errors.

Over the Mississippi Gulf coast region Yerramilli et al. (2010) studied a moderately severe ozone episode with ozone values exceeding 80 ppbv using WRF/Chem and inferred that the YSU PBL scheme together with the NOAH land surface physics scheme produced best results for both meteorological and chemical species. Air quality simulations are usually performed over periods of severe and very severe pollution episodes which are often associated with weak synoptic conditions and local scale circulations (e.g., Hurley and Manins, 1995). However, it is also important to study how well the air quality models perform under different weather conditions especially under stronger advective and topographic flows. For instance, Goncalves et al. (2008) studied the photochemical pollutants during summer time over the southern Mediterranean region using ARW/CMAQ and inferred that the transport of ozone precursors by advective flows sets the location of the maximum O_3 surface mixing ratios during midday.

In this study an attempt has been made to examine the evolution of surface ozone and other precursor emissions like NO_x over the Mississippi Gulf coast region using WRF/Chem, an online chemistry model. We are motivated to take up this work to study the performance of WRF/Chem in the simulation of moderate ozone episodes in the region that have occurred during summer condition and the results from this study could provide useful information of ozone formative meteorological processes to air quality regulatory agencies and health administrators. The summer climate in the study region is characterized with strong land–ocean thermal gradients and the resulting mesoscale Gulf breeze circulation which sets in under weak synoptic winds. Two cases of moderately severe ozone episodes in June–July 2006 during summer with sufficient observations were selected to assess the model performance.

2. Methodology

2.1. Brief description of model

The Weather Research and Forecasting – Chemistry model (WRF/Chem) is a new generation regional air quality modeling system developed at NOAA (National Oceanic and Atmospheric Administration) (Grell et al., 2005). The version of WRF/Chem used in this study is 3.1. Its meteorological model, Advanced Research WRF (ARW) is a mesoscale weather model developed by NCAR (Skamarock et al., 2008) and other research institutes in U.S. It consists of fully compressible non–hydrostatic equations, terrain following vertical coordinate and staggered horizontal grid. The model has several options for spatial discretization, diffusion, nesting, lateral boundary conditions and parameterization schemes for sub–grid scale physical processes. The physics consists of microphysics, cumulus convection, planetary boundary layer turbulence, land surface, long–wave and short–wave radiation. The chemistry module of WRF/Chem treats the processes of transport, wet and dry deposition, chemical transformation, photolysis, aerosol chemistry and dynamics. Both the meteorological and air quality components in WRF/Chem use the same transport scheme, the same horizontal and vertical grids, the same physics schemes and the same time step for transport and vertical mixing. The model has several options for chemistry, aerosol and photolysis schemes which are described by Grell et al. (2005).

2.2. Ozone episodes

From analysis of air pollution records of the last few years, two moderately severe air pollution episodes of ozone formation between 8–11 June 2006 and 18–22 July 2006 in the study region are identified. The surface ozone levels exceeded 80 ppbv during this period in the US Central Gulf Coast region. The hourly averaged surface ozone concentrations during the above episodes at eight air monitoring stations in Central Gulf Coast covering Mississippi (MS), Alabama (Al) and Louisiana (LA) are shown in Figure.1. These stations are Pascagoula and Gulfport (GPORTYC) representative of the coastal region; Hernando and Tupelo (TUPELOAP) representative of inland Northern Mississippi; Natchez Hardy and Cleveland located along Mississippi River in western Mississippi; Jackson (JACKSF19) and Meridian in the central and eastern Mississippi which fall in the study domain. Prior to the episode, the surface ozone concentrations were low on 7 June (about 50–60 ppbv) which increased to 80 ppbv at several sites on June 8 and to above 80 ppbv on June 10. The ozone concentrations were above 80 ppbv over Pascagoula, Gulfport, Natchez Hardy, Hernando on June 8, over Natchez Hardy and Gulfport on June 9, over Pascagoula, Gulfport, Cleveland, Natchez Hardy, Jackson, Meridian on June 10. All the other sites in the study region showed ozone concentrations of 70–85 ppbv between June 8 and 10. It is also found that the daily maximum 8–hour average ozone mixing ratios ranged between 67 to 84 ppbv at several monitoring stations and a considerable number of stations had above 80 ppbv during the three–day period. Similarly, the ozone concentrations exceeded 75 ppbv at stations Cleveland, Hernando, Natchez Hardy, Pascagoula, Tupelo, Gulfport on July 21, 2006 and the 8–hour ozone values exceeded above 60 ppbv in the period July 18–21, 2006 (Figure 1b). Although these periods do not characterize a very severe ozone episode, they are considered important as the 8–hour ozone values exceeded 60 ppbv, a threshold which can seriously affect people suffering from respiratory deficiencies (Simpson et al., 1997; Giorgi and Meleux, 2007) and therefore indicate moderate severe ozone pollution for human health.

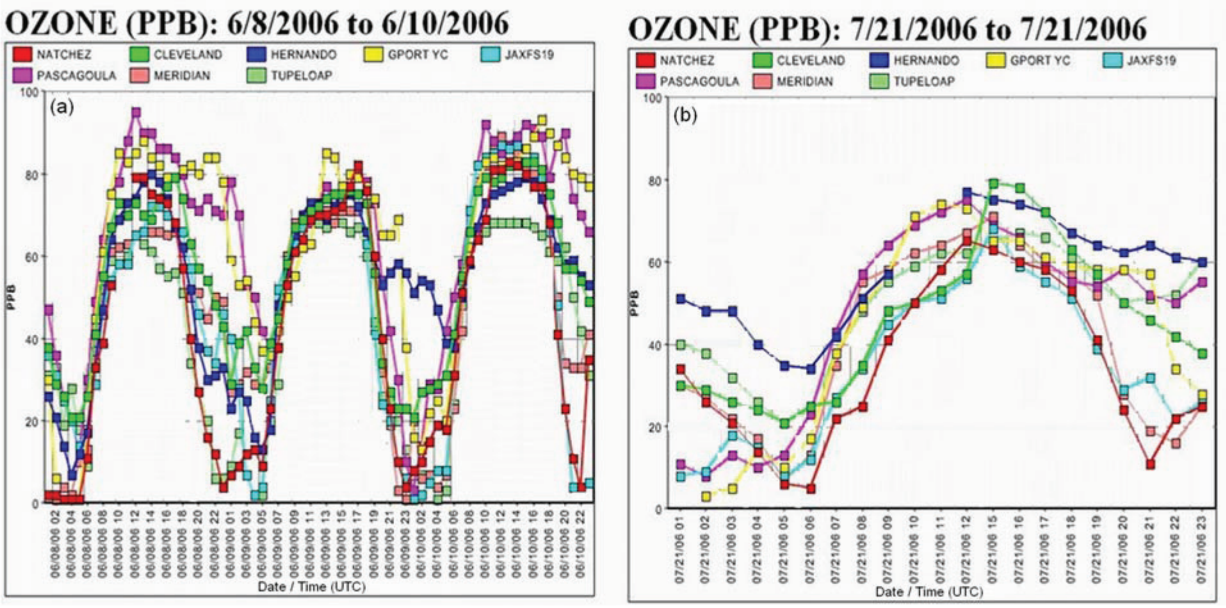

Figure 1. *Time series of hourly concentrations of O_3 at 8 air quality monitoring stations in MS Gulf coast* ***(a)*** *for 8-10 June 2006 and* ***(b)*** *for 7 July 2006. Concentration values are given in ppb.*

The study period falls in summer synoptic situation with moderate pressure gradients. Prevailing synoptic conditions on June 8, 2006 indicated presence of a low pressure system (1 005 hPa) over Atlantic Ocean near the east coast and a high pressure system (1 014 hPa) over land region of Arkansas State. Strong winds (about 15 to 20 m s^{-1}) of near cyclone intensity on the east coast and weak to moderate westerly/northwesterly winds of 3–5 m s^{-1} over the Southeast US covering Louisiana Mississippi, Alabama states have prevailed. This pressure pattern and moderate winds from northwest seem to have restricted the development of local gulf breeze and its prevalence across the coast. During July 2006 a high pressure system (1 005 hPa) prevailed over most of US associated with moderate winds. The above periods are of interest to study the ozone levels as they coincide with summer as well as moderate winds (~5 m s^{-1}) and with a good number of monitoring observations available for model validation. The typical summer weather pattern in the Central Gulf coast is characterized with diurnal ranges of air temperature as 18–35 °C, relative humidity as 35–85% and wind speeds of 1–5 m s^{-1}.

2.3. Model configuration and initialization

The WRF/Chem model is designed to have three nested domains, the outer domain covering a fairly large region of Central Gulf Coast and the inner 3rd domain covering the Mississippi coast with 4 km fine resolution (Table 1, Figure 2a). The model domains are centered at 32.8°N, –87.5°E with Lambert Conformal Conic (LCC) projection. The grid spacing's for the domains are 36 km, 12 km and 4 km respectively and the corresponding grid sizes in the east–west and north–south directions are 56 x 42, 109 x 82 and 178 x 136 respectively. A total of 31 vertical levels with 10 levels in the lower atmospheric region (below 800 hPa) are considered in the model. The inner domains 2 and 3 are two–way interactive. Terrain, land use and soil data are interpolated to the model grids from USGS global elevation, vegetation category data and FAO Soil data with suitable spatial resolution for each domain (5',2' and 30" for domains 1, 2 and 3 respectively) to define the lower boundary conditions. The model physics schemes as Lin micro–physics (Lin et al, 1983); Goddard short–wave (Chou and Saurez, 1994) and RRTM long–wave (Mlawer et al., 1997) atmospheric radiation schemes; and new Grell convective scheme (Grell, 1993) (only for domains 1 and 2) are chosen and are held constant for all experiments. Of the various physical processes, the PBL and land surface physics parameterizations control the variations of wind, temperature, humidity and mixing height in the lower atmospheric region and in turn the simulated air quality. To test the model sensitivity to PBL and LSM schemes, a series of experiments were conducted with different combinations of PBL and LSM parameterizations.

Three PBL schemes, namely Yonsei University (YSU) PBL scheme (Hong et al., 2006), Mellor–Yamada–Janjic scheme (MYJ) (Janjic, 2001), and Asymmetric Convective model (ACM) (Pleim, 2007a; Pleim, 2007b) that differ in the treatment of turbulent diffusion are alternatively tested. In the YSU PBL scheme, the vertical diffusion is calculated using a first–order diffusion formu–lation with inclusion of counter gradient terms for large scale convective eddies based on surface heat flux. The diffusion coefficients are determined for stable and unstable conditions separately following the similarity considerations based on stability functions. The eddy diffusivity coefficient for momentum is a function of the friction velocity and the PBL height, while those for temperature and moisture are computed using a Prandtl number relationship. An entrainment layer is explicitly calculated in the PBL top proportional to the surface buoyancy flux. The MYJ is a prognostic turbulent kinetic energy (TKE) scheme with local vertical mixing. The boundary layer turbulent fluxes are the turbulent perturbations (u',v',θ',q') with the perturbations in the vertical wind (w') associated with small–scale turbulent motions in the atmosphere. The eddy diffusivity coefficients (K) are parameterized in terms of a length scale of mixing and TKE, K is usually different for momentum (Km) and for heat and water vapor (Kh) (Janjic, 1990; Janjic, 1996; Janjic, 2001). The ACM is similar to Blackadar high resolution scheme available in MM5 model with a modifi–cation that the non–local diffusion due to large convective eddies is applied only for convective unstable regimes and switched off for stable regime. The eddy diffusion coefficients are determined based on boundary layer scaling formulation in terms of friction velocity, PBL height and stability function (z/L) within the PBL and using local wind shear and stability above PBL. The friction velocity and the surface exchange coefficients for heat, moisture and momentum are calculated with the Monin–Obukhov surface layer scheme by the YSU, ACM schemes and with Janjic Eta Monin–Obukhov surface layer scheme by the MYJ scheme. Land–surface models compute heat and moisture fluxes at the land surface and hence influence the estimation of PBL height. The LSMs used in the study are the multilayer soil (SOIL) scheme (Dudhia, 1996), the

Table 1. *Details of the grids and options used in the WRF/Chem model*

Dynamics	**Primitive equation, non–hydrostatic**		
Vertical resolution	**31 levels**		
Domains	**Domain 1**	**Domain 2**	**Domain 3**
Horizontal grid spacing	36 km	12 km	4 km
Grid points	54 x 40	109 x 76	187 x 118
Domains of integration	98.00°W–72.77°W 22.93°N – 39.47°N	94.86°W –79.56°W 26.49°N – 36.33°N	92.5°W – 84.60°W 28.39°N – 33.66°N
Radiation	Goddard scheme for shortwave, RRTM scheme for long–wave		
Sea surface temperature	NCEP FNL analysis data		
Cumulus convection	New Grell scheme on the outer grids domain 1, domain 2		
Explicit moisture	Lin scheme		
PBL turbulence	Hong scheme (Yonsei State University PBL), Mellor–Yamada–Janjic (MYJ), Asymmetric–Convective model (ACM)		
Surface processes	5–layer soil model, Noah LSM, Rapid Update Cycle LSM (RUC)		
Chemistry	RADM gas–phase chemical, Madronich Photolysis		

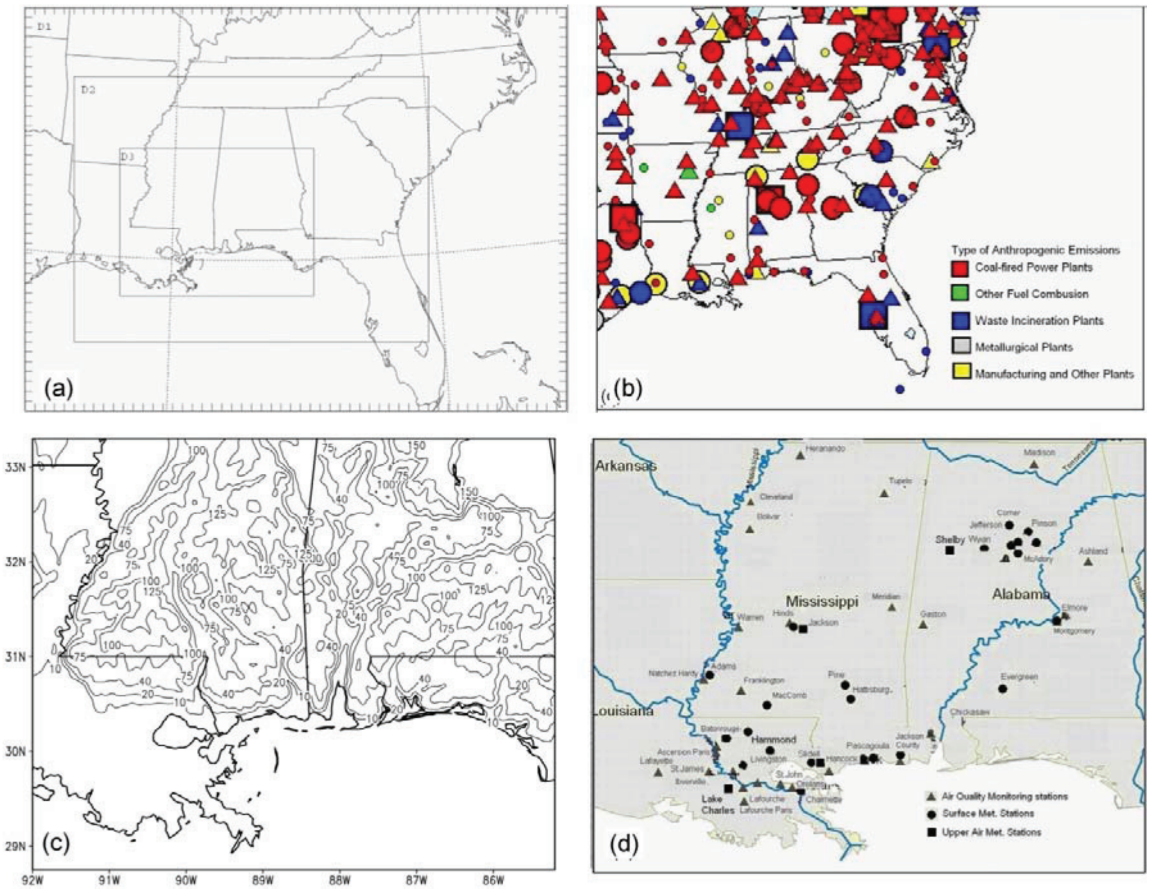

Figure 2. *Details of study region with **(a)** Model domain configuration used in WRF/Chem, **(b)** distribution of major anthropogenic sources in and around Mississippi, **(c)** terrain elevation in meters in the model inner domain and **(d)** distribution of monitoring stations.*

NOAH scheme (NOAH LSM) (Chen and Dudhia, 2001), Rapid Update Cycle scheme (RUC LSM) (Smirnova, 2000) and the Pleim–Xiu scheme (PX LSM) (Pleim and Xiu, 1995). The 5–layer soil model solves the thermal diffusivity equation with 5 soil layers. The energy budget includes radiation, sensible and latent heat fluxes. It treats the snow–cover, soil moisture fixed with a land use and season dependent constant value. The NOAH LSM treats soil and vegetation effects with the use of time dependent soil fields through a 4–layer soil temperature and moisture model and includes canopy moisture and snow–cover prediction. The RUC LSM has a high resolution soil model (6 layers) and includes the effects of vegetation, canopy water and snow. The PX LSM includes a 2–layer force–restore soil temperature and moisture model and considers evapotranspiration, soil evaporation, and evaporation from wet canopies. The PX scheme is generally coupled to the ACM PBL. A set of 10 numerical experiments are conducted with alternative PBL and LSM combinations (YSUSOIL, YSUNOAH, YSURUC, MYJSOIL, MYJNOAH, MYJRUC, ACMSOIL, ACMNOAH, ACMRUC, and ACMPX) for both the cases of simulation.

The chemistry options used in the model are the Regional Acid Deposition Model version 2 (RADM2) gas–phase chemical mechanisms (Chang et al., 1989; Stockwell et al., 1990) and Madronich photolysis scheme (Madronich, 1987). For the present study no aerosol module is included. The model chemistry is initialized with the default profiles for chemical species available with the model. A spin up time of 12 h is used for the chemistry to be consistent with the ambient conditions following the past studies (Fast and Zhong, 1998; West et al., 2004; De Foy et al., 2006; Zhang et al, 2009) which demonstrated that the WRF/Chem simulations are not very sensitive to the initial chemical conditions. The initial and lateral meteorological boundary conditions necessary for the meteorology module are defined from the National Centers for Environmental Prediction (NCEP) Final Analysis (FNL) data available at 1° x 1° resolution and at temporal resolution of 6 hours. The local standard time followed in the study region is the Central Standard Time (CST) of US. The model is initialized at 00 UTC, June 8, 2006 and integrated for 72 hours for the case 8–10 June 2006 and is initialized at 00 UTC, June 18, 2006 and integrated for 96 hours for the case 18–22 July, 2006. The model boundary conditions are updated every 6 hours from the FNL data during the simulation period.

2.4. Data

The anthropogenic emissions data is taken from the U.S. Environmental Protection Agency (EPA) National Emissions Inventory (NEI) 2005. This data consists of area type emissions on a structured 4 km grid and point type emissions at latitude and longitude locations. The data is interpolated to model grids using the emissions processing program available with WRF/Chem. Major anthropogenic emission sources from this inventory in and around Mississippi State are shown in Figure 2b. From this inventory it is noted that large coal fired power plants are situated in the western Alabama, Mississippi Gulf Coast, south–east Arkansas, northeast Louisiana and a few other plants are located in northwest, central and southern Mississippi. The biogenic emissions are calculated online using the scheme of Guenther et al. (1993, 1994). The interpolated terrain elevation from the USGS arc 30 sec data over the fine domain is shown in Figure 2c. Elevation above mean sea level (AMSL) in the study area are 10 to 20 m along the Gulf coast, 40 to 75 m in the southern Mississippi, 100 to 125 m in the central and northern Mississippi, 10 to 20 m in eastern Louisiana, 20 to 40 m in western Louisiana and 75 to 125 m in central and northern Louisiana respectively.

Meteorological observations for model comparison were taken from the NCEP ADP Global Upper air and Surface observation data set, automated weather stations data over Louisiana from Louisiana Agriclimatic Information System (http://www.lsuagcenter.com/weather) and surface reports, upper air soundings from University of Wyoming (http://weather.uwyo.edu). The model performance was evaluated for simulations of the innermost domain of 4 km resolution. About 275 surface meteorol–ogical observations and 4 upper air soundings from the study region were used in the model evaluation. The air quality observations were obtained from Aerometric Information Retrieval System (AIRS)– Air Quality System (AQS) (http://www.epa.gov/air/data/index.html). A few stations employed for visual compa–risons of meteorological fields and all air quality monitoring stations used in model evaluation are shown in Figure 2d. Qualitative and quantitative comparisons are made to assess the WRF/Chem simulated fields. For the quantitative analysis wind speed, wind direction, temperature and relative humidity at the surface (10 m or 2 m above ground level), 925 hPa and 850 hPa levels are used. The statistical metrics used in the present analysis include Pearson correlation coefficient (r), mean error or Bias (B), Mean Absolute Error (MAE) and Root Mean Square Error (RMSE) as used in air quality assessment (Willmott, 1982; Hanna, 1994; Shafran et al., 2000; Cheng and Steenburgh, 2005).

3 Results and Discussion

3.1. Results from sensitivity experiments

Results of model simulated meteorological fields and chemical species from experiments with different combinations of land surface and PBL parameterizations are discussed first to determine the best model configuration for the prediction of air quality parameters.

Meteorological Fields. Winds, temperature, humidity, turbulent fluxes, PBL height and their spatial variations assume significance in the air quality and dispersion phenomena. They characterize the transport, atmospheric stability and diffusion. The simulation of these fields and their sensitivity to different PBL–LSM options are analyzed for the 4–day simulation (July 18–22, 2006). Time series of surface meteorological variables from each of the 10 sensitivity experiments are compared with observations at twelve stations (Hammond, Mobile, Evergreen, Pascagoula, Jackson Thompson, Hattiesburg, Pine, Natchez Hardy, Kessler and Slidell) to under–stand how the model has simulated their diurnal trends and magnitudes.

Temperature, humidity, clouds and short–wave radiation influence the formation of photochemical species. Proper simulation of clouds is especially important as it will affect the estimation of photolysis rate in the model. As the considered air quality episodes belong to dry weather conditions with no significant clouds, model cloud effects are not considered important for the present study. Surface temperature, being proportional to the heat flux, has direct impact on convective turbulence and PBL vertical growth. It influences PBL mixing and diffusion of pollutants. Accurate simulation of air temperature ensures to some extent the associated PBL structure and diffusion. The diurnal temperature cycle and its mean are reproduced well by all the experiments at all the stations (Figure 3). Generally the model has slightly underestimated the daytime temperature (cold bias) and overestimated the night temperature (warm bias) at many stations. The experiment YSUSOIL has produced the highest temperatures and ACMPX the lowest temperatures. The simulation cases YSUSOIL, ACMSOIL, ACMNOAH and ACMRUC reproduced the diurnal range and magnitudes of surface air temperature at most locations. A warm bias in the night temperature is noted with YSUNOAH, YSURUC, MYJSOIL, MYJNOAH, MYJRUC, ACMPX, at many locations. In general the multilayer soil model tends to produce relatively higher temperatures than the other land surface schemes. On the average, the day temperature is underestimated by about 5% and the night temperature is overestimated by about 8%.

The daytime RH is overestimated at Natchez Hardy, Macomb, Jackson Thompson, Pine whereas it is well simulated at all other stations. In general there is a dry bias in the model during night conditions and humid bias during daytime. The magnitude of RH, considering 24–hours, is also well simulated for Hammond, Ever–green, Pine, Natchez Hardy, Slidell, Hattiesburg and Jackson Thompson and is over estimated at other stations (not shown). The model relative humidity is overestimated by about 12.5% on the average considering both coastal and inland stations. The model's inability to reproduce the magnitude of the observed extreme values at some monitoring sites could be attributed as due to the grid cell volume averaging and the resulting smoothening effects.

The model has produced the trends and diurnal range in wind speed at most locations (Figure 4). Time series of wind speed at 10 m height shows that all the simulations indicate deviations in diurnal wind speed evolution. Wind speed is well simulated at Pascagoula, Hammond, Gulfport, Mobile, Hattiesburg, Kessler, Slidell stations. The wind speed is reasonably estimated during day time at Gulfport, Hattiesburg, Pascagoula, Jackson Thompson, Hammond, Pine, and Kesler stations, overestimated at Natchez Hardy, McComb, Mobile and Jackson Thompson. It is over–estimated in the night time at most locations. Overestimation of wind speed by WRF during the night conditions has been reported in earlier studies also (e.g., Cheng and Steenburgh, 2005; Borge et al., 2008; Roux et al., 2009). In particular, the experiments YSURUC, MYJSOIL, ACMSOIL, and MYJRUC overestimated the wind speed at many locations while YSUNOAH, ACMNOAH, and ACMPX produced better estimations of wind speed and its diurnal range at most locations.

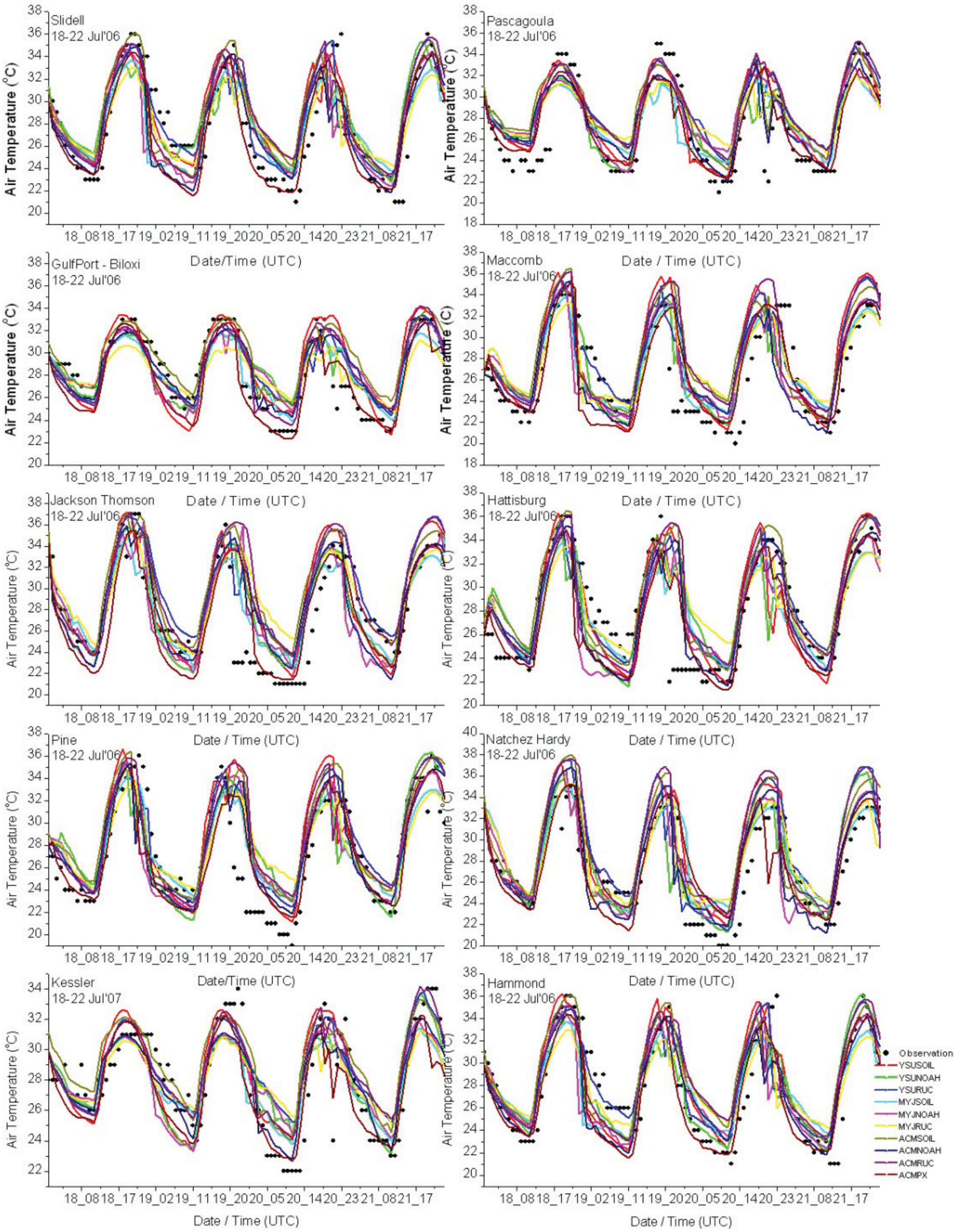

Figure 3. *Time series of simulated surface air temperature (°C) along with observations at a few surface weather stations in the model fine domain for July 18–22, 2006.*

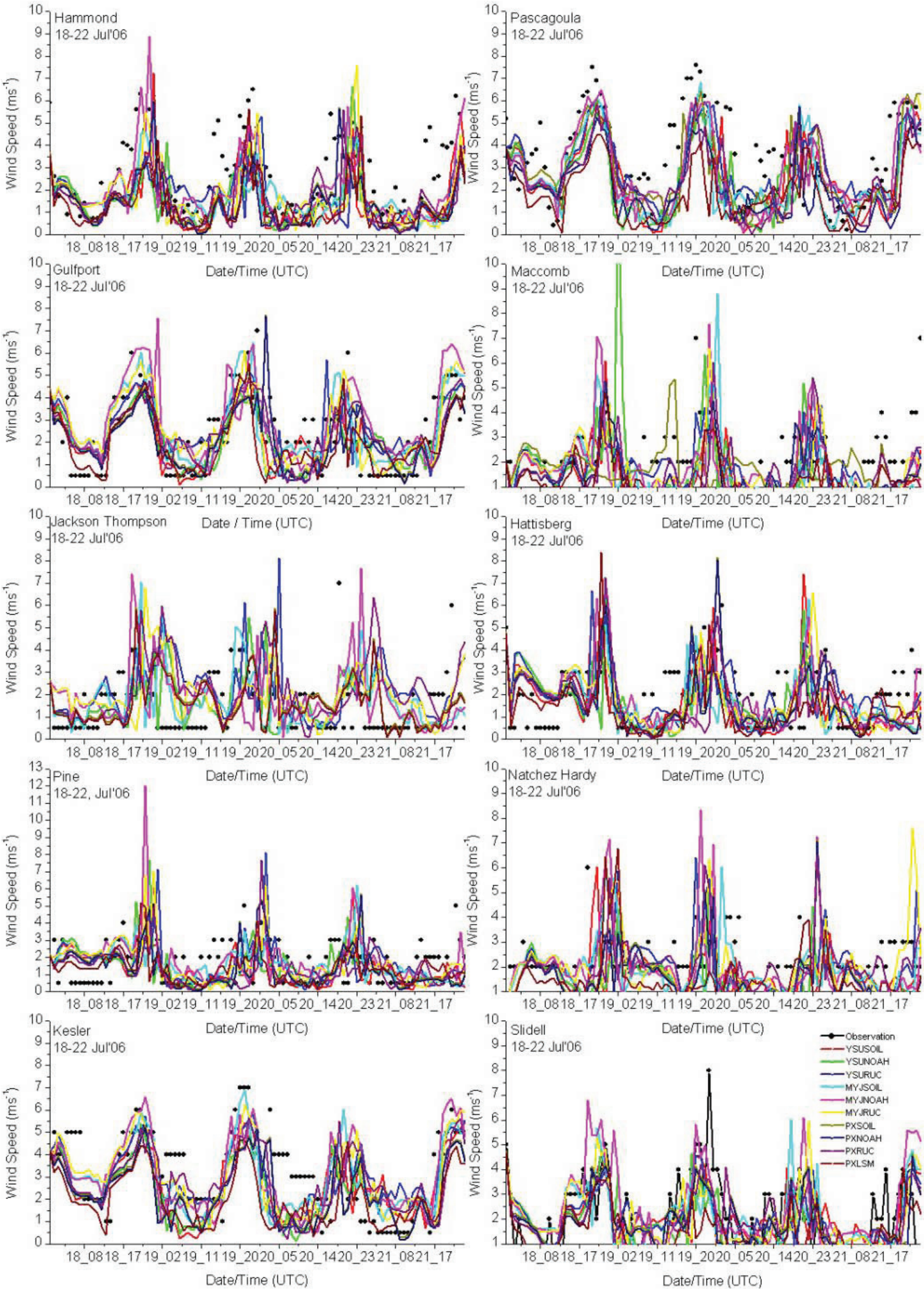

Figure 4. *Time series of simulated 10 m wind speed (m s^{-1}) along with observations at a few surface weather stations in the model fine domain for July 18–22, 2006.*

Differences in simulated wind speeds using different PBL types is due to the variation in parameterization of turbulence transfer coefficient in the three schemes and the way surface fluxes delivered by the surface layer schemes (Hu et al., 2010). The eddy diffusion coefficient is determined from predictive turbulence kinetic energy (TKE) and a length scale in MYJ scheme and from friction velocity, PBL height in YSU and ACM schemes. On the average, wind speed is overestimated by 12%. Wind direction and its diurnal trends are well simulated at most locations from all experiments. It is reasonably well simulated for the stations Pascagoula, Pine, Natchez Hardy, McComb, Hammond, Mobile, Hattiesburg stations whereas some deviations are found in the case of Evergreen, Gulfport, Slidell, Jackson Thompson and Kessler. The experiments ACMSOIL, MYJNOAH, ACMRUC, and ACMPX produced differences up to a maximum of 30 degrees in wind direction at several stations. Overall, the experiments of YSUNOAH, MYJSOIL, and YSUSOIL simulated the wind direction better than others. Time series of simulated PBL height from different exper–iments along with the value determined from radiosonde obser–vations at Jackson Thompson and Slidell stations are presented in Figure 5. The PBL height is estimated from available vertical soundings using Richardson number (RiB) with a critical value of 0.25. The model could simulate the morning 06 CST (12 UTC) and evening 18 CST (00 UTC) PBL height matching with observations. However, the experiments YSUSOIL, YSUNOAH, YSURUC, MYJSOIL produced relatively deeper boundary layer (~2 200 m at Jackson Thompson and ~2 000 m at Slidell for July 18–22, 2006); MYJNOAH, ACMSOIL, ACMNOAH, ACMRUC produced relatively shallow boundary layers (~1 600 m at Jackson Thompson and ~1 200 m at Slidell) while others produced intermediate boundary layers. As noted earlier, the soil model has produced relatively higher surface air temperatures which has resulted in higher boundary layer growth by enhancement of convective turbulence with YSUSOIL, MYJSOIL experiments. The YSU and ACM PBL schemes have a tendency to produce deeper boundary layers as has been shown in earlier studies (e.g., Hu et al., 2010) because of the prediction of higher temperatures and lower moisture in the lower atmosphere during daytime due to stronger vertical mixing and stronger entrainment at the top of PBL. The PBL height is also estimated as a function of critical Richardson number from vertical temperature and wind distribution in YSU and ACM schemes and from the vertical TKE distribution in the MYJ scheme.

Statistical evaluation of model simulations (June 8–11, 2006; July 18–22, 2006) was made through comparison with corresponding observations for temperature, relative humidity, wind speed and wind direction at the surface, 925 hPa and 850 hPa levels. Pearson correlation coefficient (r), mean error or bias (B), mean absolute error (MAE), and root mean square error (RMSE) values were computed for different experiments and presented in Table 2. The statistics were computed for all the sites at which surface data are available as well as four upper air stations in the fine grid domain. For air temperature, YSUSOIL, YSUNOAH, YSURUC, MYJSOIL, ACMRUC and ACMPX simulations gave relatively higher correlations (0.516–0.564), and lower BIAS (–0.02 to –0.50 °C), lower MAE (1.187–1.338 °C), lower RMSE (1.443–1.61 °C) than other experiments and YSU PBL scheme with 5– layer soil model had the least error. For RH the experiments YSUSOIL, ACMSOIL, YSUNOAH, ACMNOAH, YSURUC and ACMRUC yielded higher correlations (0.342–0.471), low BIAS (6.576–9.282), low MAE (6.194–9.282) and low RMSE (11.83–16.02), of which YSUSOIL, ACMRUC and YSUNOAH produced the least error metrics. Although NOAH, RUC and PX land surface models are expected to provide better simulation of the diurnal temperature variations due to better estimation of surface heat and moisture fluxes, their performance in the present study were constrained with the use of climatological values of soil moisture and soil temperatures. For wind speed, the experiments YSUNOAH, MYJNOAH, YSURUC, ACMRUC and ACMPX yielded higher correlations (0.302–0.403), lower values of BIAS (0.04–0.248 m s^{-1}), MAE (1.224–1.267 m s^{-1}) and RMSE (1.5–1.575 m s^{-1}) (Table 2) and YSUNOAH produced the best simulation with least error metrics. Statistical evaluation of wind direction is complicated as large errors are likely to arise whenever wind fluctuations occur around 0°/360° in model and observed values. Hence, in the present study the u–wind, v–wind components from model and observations are compared. The mean of the statistics for the u, v wind components is taken as a measure of model performance for wind direction. For u, v winds the model runs YSUSOIL, MYJSOIL, YSUNOAH, MYJRUC, ACMPX yielded better statistics with correlations (0.39–0.5), BIAS (–0.07–0.46 m s^{-1}), MAE (1.547–1.756 m s^{-1}) and RMSE (1.814–2.047 m s^{-1}) respectively. Of these experiments, YSUNOAH and ACMPX produced the highest correlations and lowest BIAS, MAE, RMSE and thus provide the best statistics for wind direction. Thus, among the three PBL schemes the YSU PBL has performed better than the MYJ and ACM schemes with higher correlation, lower bias, lower MAE and RMSE for the meteorological variables of temperature, humidity, wind speed and direction. Among the three LSM schemes, SOIL scheme has higher correlation, lesser BIAS for temperature and relative humidity whereas the NOAH

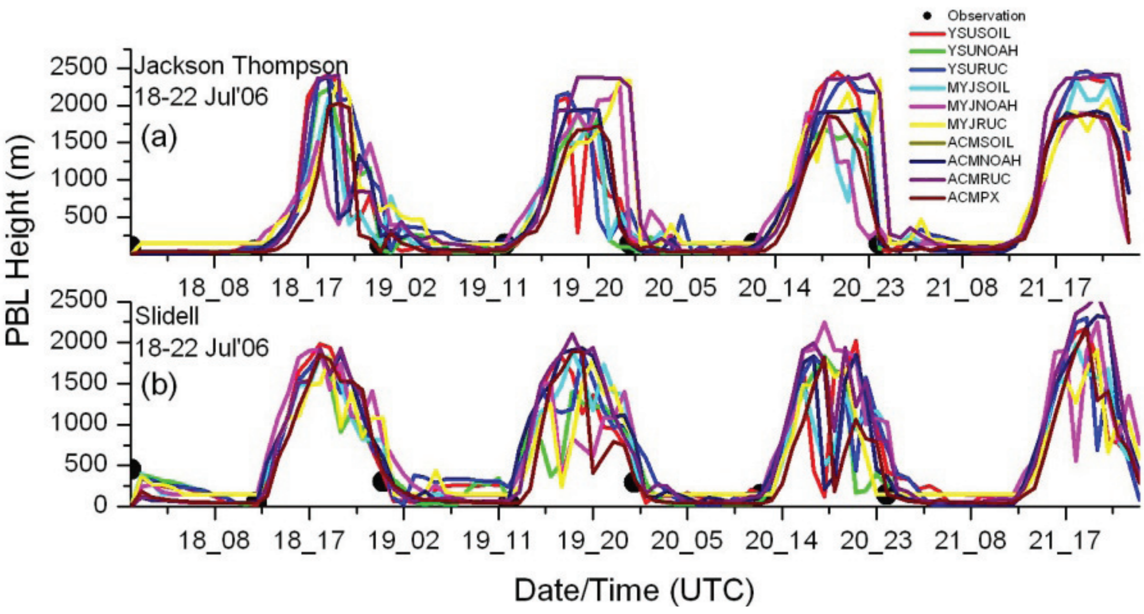

Figure 5. *Time series of simulated PBL height (m) along with values derived from Radiosonde observations (shown in dots) at **(a)** Jackson Thompson and **(b)** Slidell stations.*

scheme has lesser bias and errors for wind speed with nearly same values as of SOIL scheme for temperature and humidity. Considering all the error metrics, YSUNOAH and YSUSOIL experiments produced the best simulations of meteorological variables and YSUNOAH slightly better than YSUSOIL combination.

Table 2. *Model statistics for various meteorological variables from different experiments*

Parameter	Experiment	R	BIAS	MAE	RMSE
Temperature (°C)	YSUSOIL	0.564	–0.020	1.202	1.451
	YSUNOAH	0.518	–0.463	1.338	1.611
	YSURUC	0.545	0.134	1.187	1.443
	MYJSOIL	0.526	–0.858	1.609	1.845
	MYJNOAH	0.471	–0.647	1.477	1.754
	MYJRUC	0.488	–0.762	1.721	1.984
	ACMSOIL	0.444	–0.535	1.987	2.287
	ACMNOAH	0.395	–0.190	1.557	1.832
	ACMRUC	0.551	0.236	1.251	1.473
	ACMPX	0.516	–0.739	1.265	1.531
Relative Humidity (%)	YSUSOIL	0.460	6.576	9.765	11.479
	YSUNOAH	0.342	9.282	12.569	14.524
	YSURUC	0.362	6.194	10.579	12.382
	MYJSOIL	0.276	12.957	15.337	17.355
	MYJNOAH	0.269	10.834	13.898	16.068
	MYJRUC	0.284	9.902	14.392	16.317
	ACMSOIL	0.374	8.338	13.857	16.023
	ACMNOAH	0.436	9.425	12.462	14.337
	ACMRUC	0.471	6.907	10.093	11.830
	ACMPX	0.316	10.222	12.435	14.531
Wind Speed (m s^{-1})	YSUSOIL	0.268	0.041	1.334	1.630
	YSUNOAH	0.403	0.127	1.224	1.519
	YSURUC	0.307	0.231	1.301	1.592
	MYJSOIL	0.226	0.041	1.392	1.630
	MYJNOAH	0.344	0.248	1.236	1.532
	MYJRUC	0.291	0.240	1.300	1.575
	ACMSOIL	0.144	–0.134	1.371	1.662
	ACMNOAH	0.188	0.045	1.294	1.635
	ACMRUC	0.327	0.103	1.242	1.534
	ACMPX	0.302	0.039	1.267	1.575
u–/v– winds (m s^{-1})	YSUSOIL	0.495	–0.461	1.756	2.037
	YSUNOAH	0.469	–0.246	1.602	1.857
	YSURUC	0.434	–0.066	1.662	1.969
	MYJSOIL	0.492	–0.322	1.648	1.945
	MYJNOAH	0.394	–0.251	1.726	2.047
	MYJRUC	0.502	–0.385	1.712	2.012
	ACMSOIL	0.379	–0.254	1.744	2.040
	ACMNOAH	0.394	–0.074	1.817	2.133
	ACMRUC	0.429	0.229	1.640	1.985
	ACMPX	0.495	–0.071	1.547	1.814

Chemical species. Simulated hourly ozone mixing ratios at 10 m AGL (above ground level) along with observations for the episodes 00 UTC June 8–00 UTC June 11, 2006 and 00 UTC July 18–00 UTC July 22, 2006 is shown in Figure 6 for six monitoring stations (Tupelo, Natchez Hardy, Hernando, Cleveland, Jackson in Mississippi and Elmore site in Alabama). In general the model could simulate the diurnal trends of ozone at all the sites. Predicted ozone values varied among simulations using different PBL and LSM physics. Experiments ACMSOIL, ACMNOAH, ACMRUC, and ACMPX have overestimated the daytime ozone by about 15% and underestimated the night time ozone by about 12% giving a net underestimation of 9% of daily average.

Experiments YSUSOIL, YSUNOAH, YSURUC, MYJNOAH, and MYJRUC underestimated the daytime ozone by about 10% and overestimated the night time ozone by about 7% with a net underestimation of about 8% of daily average ozone. Experiment MYJSOIL underestimated daytime ozone by about 14% and over–estimated night time ozone by about 8% with a net under–estimation of 9% of daily average ozone. Of all experiments, YSUNOAH has produced both the diurnal cycle and range of ozone mixing ratios more realistically and in good agreement with observations. The standard deviation in observed ozone is found to be 24% using data of all available monitoring stations. The standard deviation of model simulated ozone is found to be 14–15% with YSU PBL, 15–16% with MYJ PBL and 16–19% with ACM PBL scheme respectively (Table 3) which indicates that the simulated time variations show lesser diurnal dispersion than the observations. The highest correlations (69 to 73%), least BIAS (–0.75 to 3 ppbv), MAE (8 to 10 ppbv) and RMSE (14 to 16 ppbv) are found with YSUSOIL, YSUNOAH, YSURUC, MYJSOIL, MYJNOAH, MYJRUC while the highest bias, MAE, RMSE are found with ACMSOIL, ACMNOAH, ACMRUC, ACMPX respectively. Overall, the simulations with YSUNOAH, YSUSOIL, and MYJNOAH provide least error metrics for diurnal ozone estimation at various sites (Table 3). For NO_2 the simulations YSUSOIL, YSUNOAH, YSURUC, MYJSOIL, MYJNOAH produced low standard deviation (2 to 3.5), high correlations (40–55%), low MAE (2.5 to 3.3 ppbv), low BIAS (–1.47 to –1.85 ppbv) and low RMSE (4.8 to 5.9 ppbv). NO_2 being an important precursor for ozone formation, relatively low errors in NO_2 estimation might have led to more accurate estimation of ozone in the above experiments. The other contributing factors are, of course, more accurate simulation of meteorological quantities in the experiments YSUSOIL, YSUNOAH, YSURUC, MYJSOIL, and MYJNOAH. Of the various experiments YSUNOAH has simulated NO_2 with high correlation, least errors and with underestimation of 10%. Comparison of statistics of experiments with different PBL schemes shows that YSU PBL is better than the MYJ and ACM schemes in ozone, NO_2 simulation. Similarly comparison of results from experiments with different soil schemes indicates that SOIL and NOAH schemes are better than RUC and PX schemes for ozone and NO_2 simulations. Thus YSUNOAH produced the best results for simulation of ozone and the precursor NO_2 over the study region for the episodes in June 2006 and July 2006.

Simulated and observed hourly averages of ozone for daytime 12–hours denoted as 1–hr average and daily maximum 8–hour average denoted as 8–hr average (following USEPA) at various monitoring stations in the study region from experiments using different combinations of PBL and LSM schemes are given in Table 4. As per USEPA, National Ambient Air Quality for Ground Level ozone is 120 ppb and 75 ppb for 1–hour and 8–hour averages. The 8–hour ozone values above a threshold value of 60 ppbv seriously affect people suffering from respiratory deficiencies (Simpson et al., 1997; Giorgi and Meleux, 2007). Model simulated 1–hr, and 8–hr average ozone for both periods (June 8–11, 2006, July 18–22, 2006) are underestimated in all the exper–iments, and the YSUSOIL and YSUNOAH experiments produced better estimation with magnitudes higher than other experiments and closer to the observations. The 1–hr ozone values are under–estimated by ACMSOIL, ACMNOAH, ACMRUC, and ACMPX by 16% for June 8–11, 2006 and by 24% for July 18–22, 2006 respectively. Similarly the 1–hr ozone values are underestimated by MYJSOIL, MYJNOAH, and MYJRUC by 3% for June 8–11, 2006 and by 15% for July 18–22, 2006 respectively. The 1–hr ozone is overestimated by

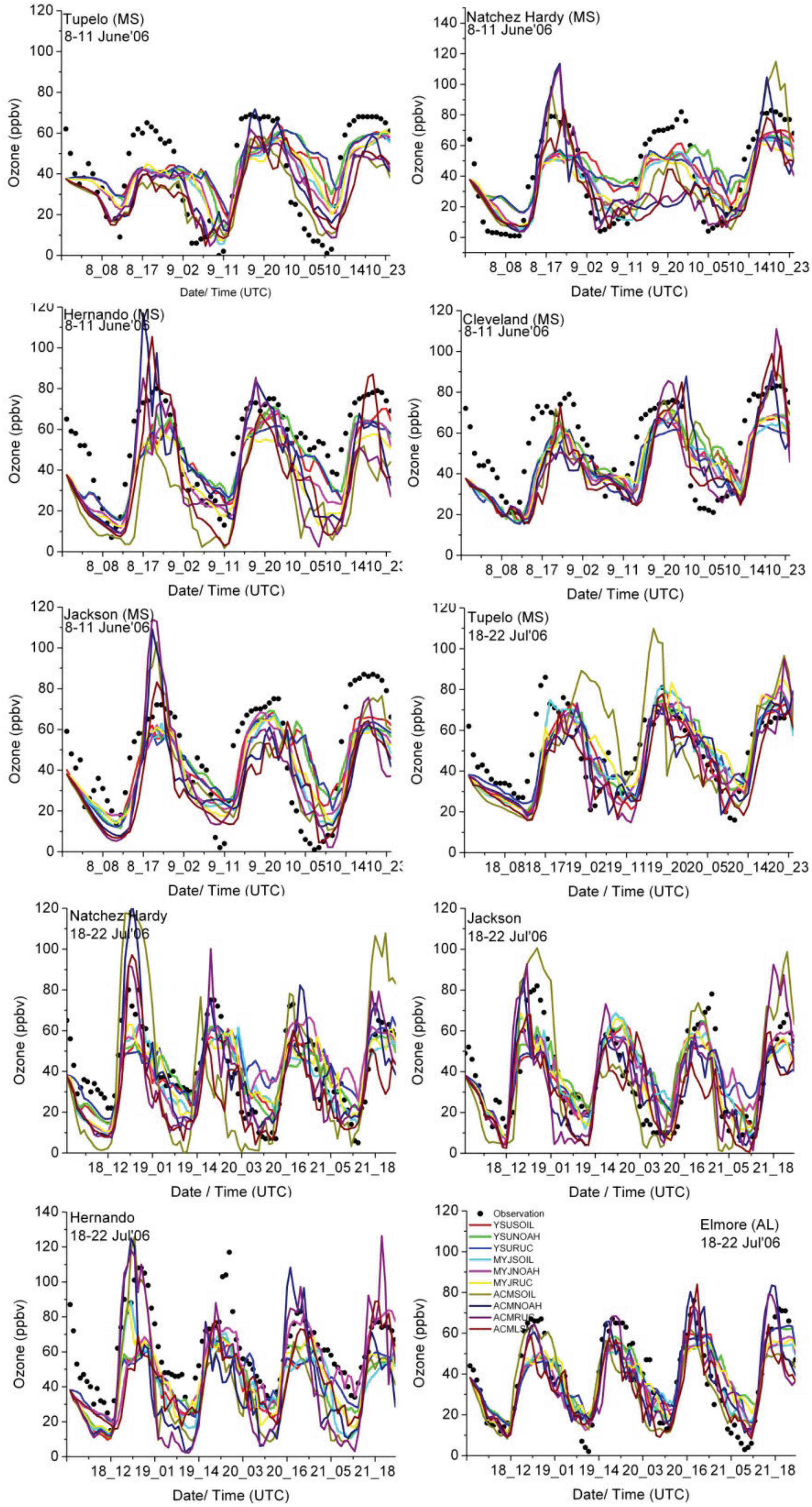

Figure 6. *Time series of simulated hourly ozone (ppbv) along with observations at a few surface weather stations in the model fine domain for June 8–11, 2006 and July 18–22, 2006.*

Table 3. *Model statistics for selected air quality species (O_3, NO_2) from different experiments*

Parameter		SD	Corr	BIAS	MAE	RMSE
Ozone	YSUSOIL	14.92	0.699	–0.350	8.63	15.831
	YSUNOAH	14.41	0.726	–1.533	8.11	14.514
	YSURUC	13.87	0.663	–0.778	9.36	15.831
	MYJSOIL	16.19	0.697	–4.22	9.94	15.498
	MYJNOAH	15.79	0.728	–2.68	9.19	14.506
	MYJRUC	15.90	0.710	–3.61	9.66	15.079
	ACMSOIL	22.64	0.652	–9.10	10.77	19.368
	ACMNOAH	19.45	0.625	–6.61	11.52	18.163
	ACMRUC	21.07	0.663	–6.65	11.10	17.669
	ACMPX	18.14	0.641	–9.72	11.86	18.816
NO_2	YSUSOIL	2.33	0.45	–1.47	3.23	5.97
	YSUNOAH	2.56	0.52	–1.87	3.12	5.31
	YSURUC	1.78	0.51	–1.69	3.21	5.68
	MYJSOIL	3.52	0.51	–1.85	2.73	4.86
	MYJNOAH	3.51	0.56	–3.13	2.74	4.87
	MYJRUC	3.31	0.42	–2.98	2.92	4.92
	ACMSOIL	4.44	0.39	–2.95	3.52	5.72
	ACMNOAH	4.25	0.42	–4.46	3.48	5.48
	ACMRUC	3.54	0.33	–3.98	3.41	5.45
	ACMPX	4.21	0.35	–4.32	3.81	5.95

3% for June 8–11, 2006 and underestimated by 3% for July 18–22, 2006 by Simulation YSUSOIL. The 8–h average ozone values are underestimated by ACMSOIL, ACMNOAH, ACMRUC, ACMPX exper–iments by 21% for both June 8–11, 2006 and July 18–22, 2006 cases. The experiments YSURUC, MYJSOIL, MYJNOAH, and MYJRUC underestimated the 8–hr ozone values by 16% for June 8–11, 2006 and by 21% for July 18–22, 2006 respectively. YSUSOIL experiment underestimated 8–hr ozone by 15% for June 8–11, 2006 and by 18% for July 18–22, 2006 respectively. The experiment YSUNOAH simulated the 1–hr and 8–hr ozone values with 3%, 10% under–estimations thus providing best simulation for ozone. These results lead us to conclude that YSU PBL scheme in combination with NOAH and SOIL land surface schemes provides the best simulations and NOAH scheme shows slight better performance than SOIL scheme. These results are similar to the meteorological predictions indicating that meteorological processes are important for the simulation of the evolution of surface ozone.

Model performance for ozone simulation. The sensitivity exper–iments with physical parameterizations of PBL and land surface physics processes have shown that the combination of YSU PBL and NOAH land surface schemes produced the best model estimates for meteorological parameters as well as for ozone and one of its precursors NO_2. This simulation is examined further to study the model performance for ozone. For this simulation (YSUNOAH) the average daytime ozone is underestimated by about 8%. The diurnal time series of simulated ozone with YSUNOAH indicates that the mean mixing ratio of ozone is reasonably well simulated, as borne out by the bias. The time variations of the diurnal cycle are also good as inferred from the high correlation coefficient. The diurnal range in ozone mixing ratio is slightly underestimated (~10%) which is probably due to underestimation of NO_2 by 10% and because of a slight cold bias in model temperature and stronger model winds. Slight underestimation of NO_2 is attributable to the applied source strength and applied chemical parameterizations. In the present study the EPA 4 km resolution emission inventory has been interpolated to model grids in the fine domain which may require even higher resolution data for more accuracy, especially for applications near the coast. Stronger winds give rise to stronger advection of precursor gases and ozone. Temperature controls the diffusion as well as the rate of chemical reactions. Lower temperatures reduce the reaction rates while also reducing the eddy diffusion, the former tends to slow down the ozone formation rate and the later tends to poor diffusion of produced ozone. Stronger advection dominates diffusion processes in the direction of flow thus leading to reduction in ozone levels. Under calm wind conditions diffusion becomes equally important as transport, however model as well as observations have shown occasional occurrence of calm winds during the simulation period so that role of advection can be considered greater than that of diffusion on the simulated ozone mixing ratios for the period of study. Model turbulent diffusivities depend on the type of PBL employed. In our sensitivity exper–iments using WRF/Chem (Yerramilli et al., 2010) it has been found that the non–local first order turbulence closure scheme YSU gives realistic vertical temperature, humidity, and wind profiles in the lower atmosphere while also producing observed mixed layer depth thus indicating better simulation of turbulent diffusion than the higher order complex diffusion schemes. With all the limita–tions of applied emission data, deficiencies in physical and chemical parameterizations the results obtained indicate model has appreciably simulated the ozone in the study region. Better performance of NOAH land surface model, even with using climatological values for soil temperature and moisture, indicates the advantages of using predicted soil temperature and moisture variables.

Table 4. *Model statistics for 1–hr, 8–hr ozone values at all stations*

8–11 June 2006	1–hr Average	8–hr Average
Observation	37.71	60.84
YSUSOIL	38.86	51.45
YSUNOAH	37.65	54.13
YSURUC	39.11	50.13
MYJSOIL	36.61	50.94
MYJNOAH	37.69	52.05
MYJRUC	36.78	51.54
ACMSOIL	29.32	50.52
ACMNOAH	33.21	48.53
ACMRUC	33.36	51.77
ACMPX	29.87	42.39
1/–22 July 2006	**1–hr Average**	**8–hr Average**
Observation	42.74	65.75
YSUSOIL	40.04	53.64
YSUNOAH	41.45	53.58
YSURUC	40.26	52.64
MYJSOIL	35.40	51.17
MYJNOAH	37.54	53.17
MYJRUC	36.46	51.58
ACMSOIL	32.81	52.26
ACMNOAH	33.30	51.58
ACMRUC	33.34	53.82
ACMPX	30.70	47.54

3.2. Surface ozone and meteorological processes

Flow fields. The meteorological processes underlying the moderately severe ozone episode in June 8–11, 2006 are examined. The transport of air pollutants is determined mainly by the atmospheric flow fields and the vertical mixing due to the diffusive processes in the turbulent boundary layer. The other influential parameters for the formation of photochemical pollutants are temperature, humidity, cloud cover and short–wave radiation. The effects of clouds are not considered important as the present case study falls in a clear sky dry weather condition. Simulated flow field at 10 m above ground level (AGL), surface temperature and relative humidity from the fine domain for the experiment YSUNOAH (which has given minimum errors in meteorological fields) for the episode June 8–11, 2006 are compared with the NAM (North American Mesoscale model) analysis data (based on observations and four–dimensional data assimilation) available at 12 km resolution (Figure 7). During the morning conditions (12 UTC/06 CST) on June 9, 2006 WRF/Chem shows northeasterly flow with light winds (about 2–3 m s^{-1}) in the central and northwestern parts of Mississippi, northeasterly flow in the northern parts of Mississippi, Alabama and northerly winds in western Alabama. Over the Gulf coast, strong northerly offshore winds prevailed in coastal Louisiana, Mississippi, Alabama and western Florida and are noted to be relatively stronger (~10 m s^{-1}) over the oceanic region. During the local daytime at 18 UTC/12 CST (Figure 7c) the wind flow over most of the land region is strong (5–7 m s^{-1}) northerly in Mississippi, Alabama and southern Louisiana. At 00 UTC (June 10)/18 CST June 9 the direction of flow is changed along the Gulf coast as seen from the onshore (Gulf breeze) winds over Louisiana, Mississippi and Alabama coast. The onshore flow is strong southerly (~10 m s^{-1}) along MS coast, southeasterly along Louisiana coast and south–westerly along Alabama and west Florida coasts. The direction of air circulation over the land gradually changed after 18 CST June 9. Relatively calm winds in Alabama and eastern Mississippi and southeasterly flow in western Mississippi and western Louisiana are identified at 06 UTC/00 CST, June 10, 2006 (Figure 7g and 7 h). The flow seems to converge along the Louisiana/ Mississippi River at 18 CST. The Gulf breeze is restricted to a few tens of kilometers along the Mississippi and Alabama coasts and is extended in Louisiana. The limited extent of sea breeze circulation, seen from simulation, is attributable to the low pressure on the east coast and the resulting moderately strong synoptic winds. The timing and strength of sea breeze is well simulated by WRF/Chem as seen from comparison with NAM data as well as the time series of winds (speed and direction) at different observation sites Pascagoula, Gulfport, Slidell (Figure 4) along the Gulf coast. Comparisons at Pascagoula, Gulfport and Slidell stations clearly show that both observations and model winds indicate strong winds blowing in southerly/southeasterly direction and that model values are in reasonable agreement with observed winds. This particular aspect of sea breeze along Gulf coast was studied in depth by the authors (Yerramilli et al., 2008; Challa et al., 2008; Challa et al., 2009) and reported that WRF simulates well the characteristics of flow field and associated shallow mixing layer along Gulf coast during sea breeze time. Simulated flow field agrees with NAM analysis, day time temperature is slightly underestimated and humidity is slightly overestimated (Figure 7c, 7d, 7e, 7f).

The simulated mixing height at 0600 CST is about 200 m over the land region and about 400–600 m over the marine region. A deep mixed layer of about 2 000 m is simulated during convective day time (1200 CST) in the land region of the domain which is noted to reduce to 1000 m near the coast. The coastal boundary layer has gradually become very shallow (200 to 600 m) as seen from results at 1800 CST. This is because of the advection of humid cold air mass from ocean and alteration of air overland. Simulated mixed layer depth is in good comparison with the estimated values form radiosonde observations at Slidell (near coast) and Jackson (central Mississippi). For this period the diurnal range of various meteorological parameters are 20–34°C for temperature, 40–95% for RH, and 0.02–0.93 Watt m^{-2} for net short–wave radiation in the study region which suggests that the local meteorological conditions are favorable for the formation of ozone during the episode.

The simulation period falls in late spring within two weeks of Summer Solstice. With weak synoptic–scale influence and near–solstice insulation, the primary effects will be essentially diurnal in terms of higher daytime ozone and localization of ozone under the influence of the local scale circulations in the study domain. Ozone forms in the lower atmosphere by a series of reactions involving the UV–radiation and precursor emissions of nitrogen oxides (NO_x) and volatile organic compounds. The local weather conditions such as winds, temperature, solar radiation, and horizontal and vertical diffusion characteristics influence the precursor mixing ratios, reaction rates, and formation, transport, and deposition patterns. Higher temperatures would lead to higher reaction rates with NO_x, VOCs and higher ozone production.

Results for both simulated as well as observed ozone mixing ratios at many sites indicated 3 peaks corresponding to daytime production and 3 troughs corresponding to night time consump–tion. The peaks in diurnal ozone mixing ratio occurred at 21 UTC (15 CST) and the minimum at 10 UTC (04 CST) at most sites. To examine the local diurnal influences on the ozone distribution, average ozone mixing ratio is estimated at four characteristic times 10 UTC (04 CST), 14 UTC (08 CST), 21 UTC (15 CST) and 02 UTC (20 CST) corresponding to the local night , morning, convective daytime and evening conditions respectively during the 3–day period of simulation. This 3–day mean ozone mixing ratio at specific times along with the 3–day mean wind flow at the respective times is depicted in Figure 8. For the purpose of comparison ozone mixing ratios <40 ppbv are considered as ”low–range”, 40–50 ppbv are considered as “considerable” and >50 ppbv as ”high”, respectively. Throughout the diurnal cycle the minimum ozone is found in the eastern Alabama, western Florida while the maximum ozone is located in the eastern Louisiana, northern and central Mississippi respectively. The simulated ozone is low over land region during the night conditions (Figure 8a) and is limited to a small region (with mixing ratio 33–40 ppbv) over the north–western parts of Mississippi. Simulated temperature is relatively higher (23–25°C), relative humidity relatively lower (20%) in the northwestern parts of Mississippi and mixing height about 200–400 m over the coastal parts at 06 CST (Figure 7). The mean wind is calm in the central parts and strong southeasterly or southerly in the northwestern parts where relatively higher ozone is simulated. The flow pattern indicates northwesterly off–shore winds along the coastal parts and adjoining ocean region.

The mean ozone pattern corresponding to the morning conditions at 14 UTC/08 CST indicates increase in ozone over a considerable land area in coastal, central and northern parts of Mississippi. One of the probable reasons for the increase in ozone mixing ratio at 08 CST is the downward mixing of O_3 from the residual layer aloft, as the nocturnal boundary layer breaks down due to surface heating and is replaced by the daytime convective boundary layer with its vigorous vertical mixing. Also, the mean wind at this time is northerly and very calm over the land region. Areas with calm winds are noted to associate with relatively higher ozone levels, the calm winds would lead to weaker advection of ozone. Considerable ozone development is noticed over the marine zone near Mississippi, Alabama and west Florida associated with wind flow from ocean region. The 3–day mean ozone levels during convective daytime condition corresponding to 15 CST (Figure 8c) and evening condition corresponding to 20 CST (Figure 8d) are relatively higher over land region than over marine region. The 3–day mean ozone at 15 CST shows the ozone is at its peak generation in the study region; the maximum ozone is located in the northern, northwestern parts and reduces gradually to the eastern land portions in Alabama and the marine region. The ozone is also relatively higher in the marine region adjacent to Louisiana and Mississippi coast. The areas with high ozone in northern, northwestern parts and coastal parts of the domain are associated with relatively higher air temperature (31–34°C) and relatively lower relative humidity (20–40%) at this time (Figure 6). The 3–day mean flow pattern at 1500 CST indicates that surface

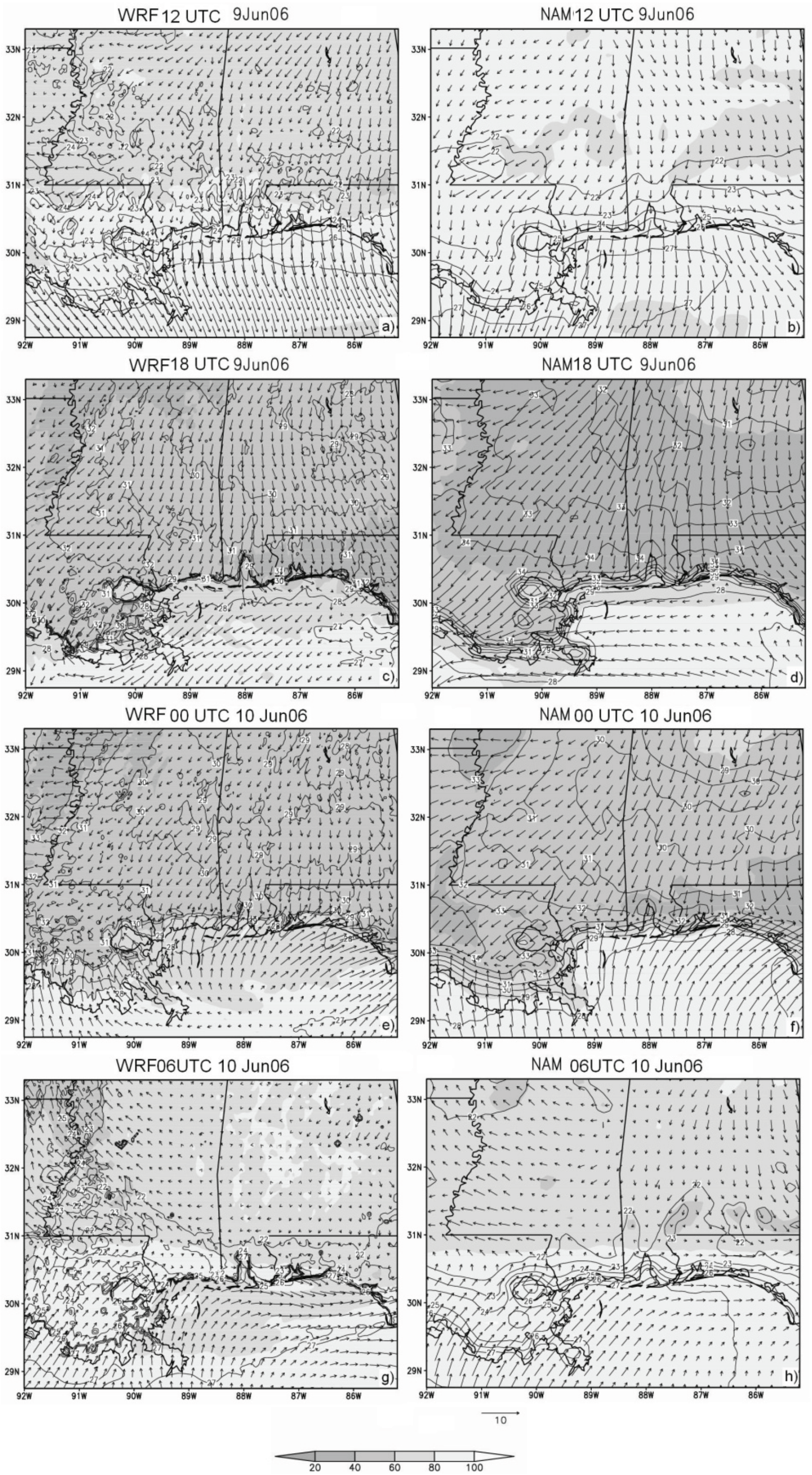

Figure 7. *Simulated spatial distribution of flow field, temperature and humidity distribution along with NAM data at 12 UTC **(a,b)**, 18 UTC **(c,d)** on June 9 and 00 UTC **(e,f)** and 06 UTC **(g,h)** June 10, 2006.*

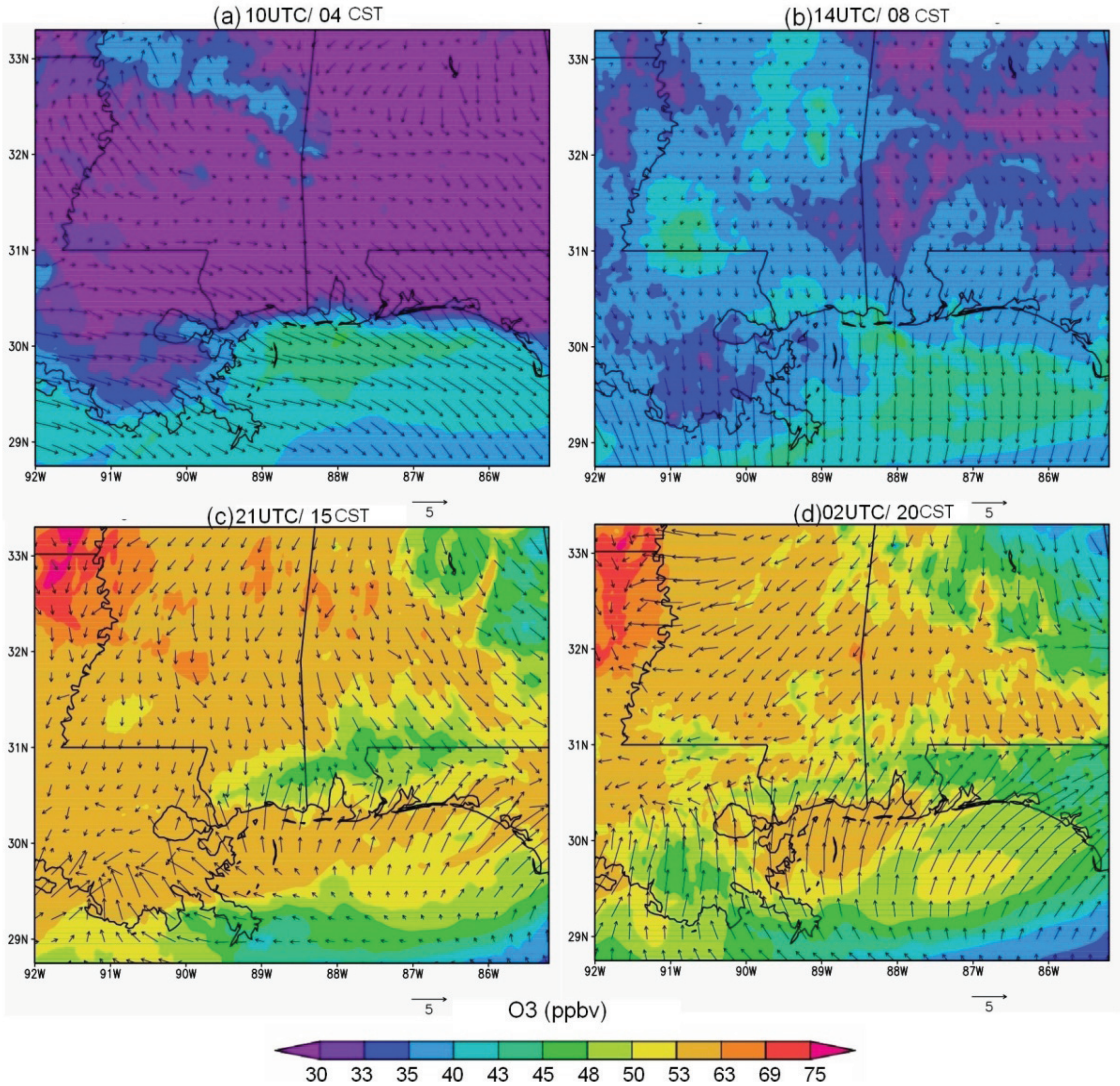

Figure 8. *Simulated spatial distribution of 3–day mean surface ozone at **(a)** 10 UTC, **(b)** 14 UTC, **(c)** 21 UTC and **(d)** 02 UTC between June 8–11, 2006 along with average wind flow. The concentration units are in ppbv.*

winds are northerly over a major land portion and strong onshore along the coast. The onshore winds at 1500 CST are due to the gulf breeze development simulated by the model. The surface air flow pattern from land and ocean regions shows horizontal conver–gence along the coastal belt. The zone of gulf breeze is noted to be associated with moderately high ozone mixing ratios (50–63 ppbv). The mean wind over the MS Gulf coast shows sea breeze development confined to about 30 to 40 miles which suggests transportation or recirculation of precursor pollutants/ozone from the marine region to the Mississippi and Alabama coasts. The possible mechanism for ozone formation over the Gulf and its subsequent inland transport can be explained as that the ozone precursors (NO_x and VOCs) are advected out to sea by the morning land breeze (northerly winds), where O_3 has then formed over the water, and the afternoon Gulf breeze transported this O_3 back onto the land. It is to be noted that many coal fired power plants are situated along the Gulf coast (Figure 2c) which contribute to this recirculation mechanism of pollutants by Gulf breeze. The ozone has gradually decayed towards the night condition as seen from the mean mixing ratio pattern in the evening time (Figure 8d). During the evening time (20 CST) north easterly/easterly mean wind flow is seen to prevail over northern and central Mississippi which converges around the pocket of highest maximum ozone in the north western parts. There are emission sources in the northern, northwestern and eastern parts, the upwind regions for this high ozone area (Figure 2c). Mean flow pattern at 20 CST suggests the possible role of transport (advection) of precursor gases from north and northeastern parts of the fine domain to the Mississippi river and its western banks causing high ozone in that region. Thus the model results indicate that the higher ozone levels in the coastal, north and northwestern parts which are related to higher temperatures and the advection under the prevailing local scale flow pattern. The mean ozone mixing ratio pattern and the mean winds suggest the role of horizontal transport of photo–chemical pollutants from north and northeast in the northwest parts of the domain and by the Gulf breeze in the southern parts of the domain during the episode. The 3–day mean distribution of ozone and vertical winds at the specific hours 10 UTC (04 CST), 21 UTC (15 CST) (corresponding to the local night and daytime conditions) in a vertical cross–section at the latitude of Jackson (32.3° N) are depicted in Figure 9. During the night time the mean ozone mixing ratio is low (30–42 ppbv) in the lower levels (below sigma = 0.964) and gradually increased upwards. The maximum Ozone build up is found in the western side between 90.5°W and 92.0°W longitudes. The vertical ozone mixing ratio gradually falls to the eastern sector. The simulated vertical winds during the night condition are weak (1–2 cm s^{-1}). A high ozone development and its vertical distribution are noted during the daytime at 15 CST. It is interesting to find that the regions with higher ozone mixing ratio are collocated with relatively strong vertical winds (2 to 5 cm s^{-1}) and the following subsidence (downward flows). The strong positive and negative vertical winds represent the well mixed atmospheric conditions and higher vertical extent of ozone under the daytime convective condition. Strong upward air flows are noted between 91° and 92° W with downward flows on the eastern side. This region with very strong upward vertical flow is marked with high ozone mixing ratio (>50 ppvb) which suggests the role of boundary layer convection and vertical mixing for the occurrence of high ozone on the northwestern parts of Mississippi along the region of Mississippi River during the episode June 8–11, 2006.

4. Conclusions

Two moderately severe surface ozone episodes in the Central Gulf Coast Region during summer, during June 8–11, 2006 and July 18–22, 2006, were studied using the fully coupled WRF/Chem air quality model. The results indicate that the model simulated the observed trends in meteorological variables, however with slight underestimation of surface temperature and humidity during day–time and overestimation during night time. It also simulated the vertical atmospheric structure and mixed layer characteristics agreeing with available radiosonde observations at Jackson and Slidell stations. A suite of experiments conducted with different PBL and land surface physics parameterizations showed that the YSU PBL together with NOAH and SOIL land surface models produces best simulation for various required meteorological quantities in air quality simulations. It has been found that WRF/Chem simulated the temperature with underestimation of 1.3°C, overestimation of wind speed by 1.2 m s^{-1} and humidity by 11%, all the error limits indicating a good simulation of meteo–rological fields. Simulated wind flow pattern agrees with the NAM analysis and shows the occurrence of sea–land breeze flow along the coast, both the timing and strength of sea breeze are found to agree with the data from surface stations at the coast though the inland extent of sea breeze is limited for the period of simulation. The simulated chemical species (O_3, NO_2) are found to reasonably match with the observations from air monitoring sites with a slight underestimation in the daytime values. The sensitivity experiments using different PBL and LSM schemes revealed that ACM scheme has overestimated the daytime ozone while YSU and MYJ schemes underestimated the daytime ozone. ACM, MYJ PBL schemes give large errors of simulated chemical species while the YSU PBL provides minimum errors. The experiment YSUNOAH well simulated the diurnal mean mixing ratio, timing of diurnal cycle as well as range in ozone mixing ratio at most monitoring stations with an overall correlation of 0.726, bias of –1.55 ppbv, 8.11 ppbv of MAE and 14.5 ppbv of RMSE which are the best statistics obtained of all experiments. The average daytime ozone is under–estimated by about 8% and peak daytime Ozone is underestimated by about 7 ppbv at different locations. The model produced 1–hr, 8–hr average ozone values agreed well with corresponding averages from observations. The slender underestimation in ozone is because of slightly stronger winds and lower temperatures simulated by the model. The spatial pattern of simulated ozone mixing ratios obtained from 3–day mean of the night time (average of 3 lows) and daytime (average of 3 peaks) conditions indicate that the maximum ozone is located in the northwestern and the marine coastal parts. The influence of local scale sea breeze flow on surface ozone could be simulated by WRF/Chem as seen from the observed and predicted mixing ratios at coastal stations. The areas with high ozone are found to be associated with relatively higher local air temperature and local flows. The buildup of columnar ozone during daytime is found to be associated with well mixed conditions as noted from strong upward and downward vertical winds in the boundary layer. The study suggests that horizontal transport of precursor pollutants and the boundary

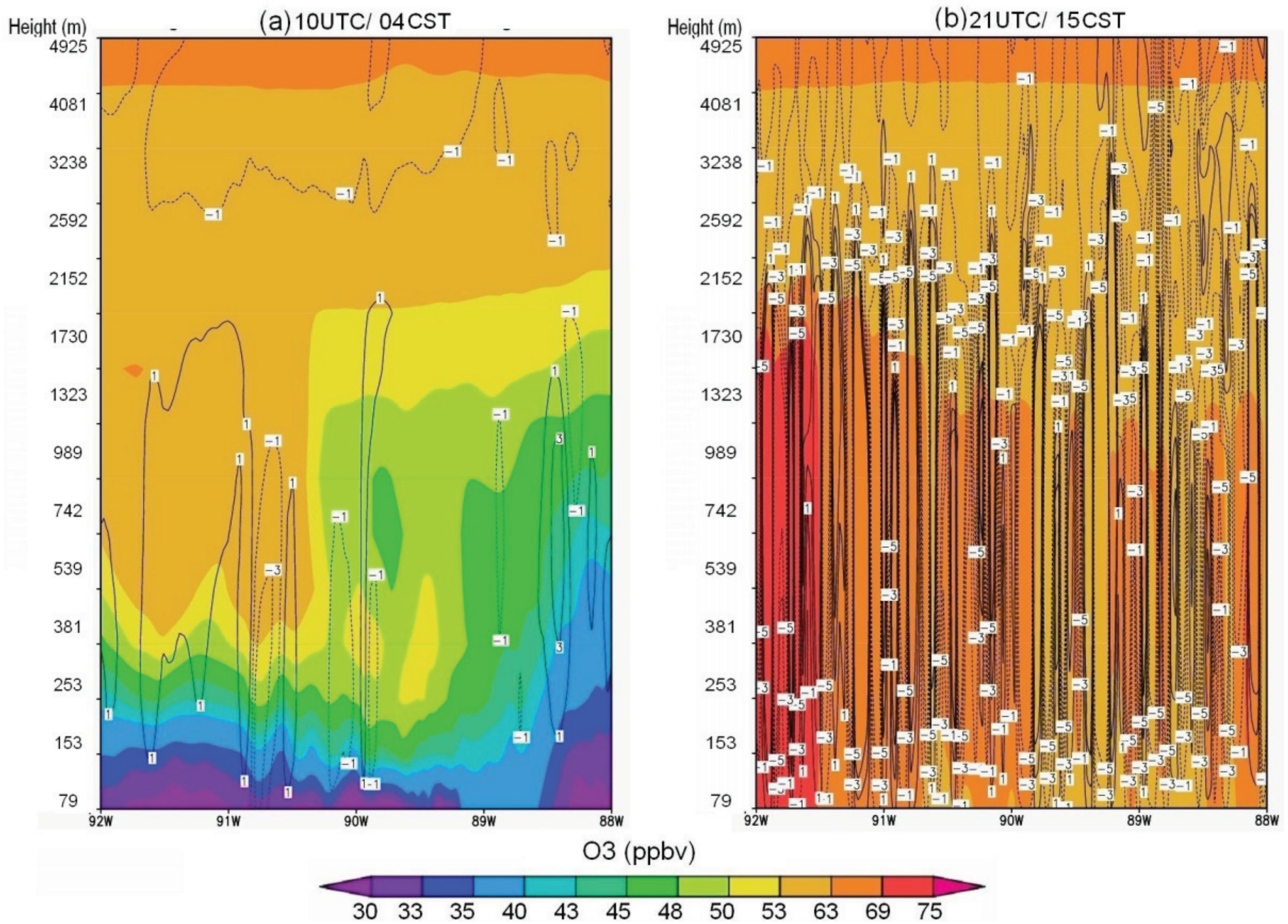

Figure 9. *Vertical cross–section at latitude of Jackson (32.3 °N) of the 3–day mean vertical velocities (in m s^{-1}) and 3–day mean ozone distribution corresponding to **(a)** 10 UTC and **(b)** 21 UTC during the episode.*

layer convective mixing (diffusion) play important role in the high ozone formation during the period. WRF/Chem model has reproduced the selected moderately severe ozone episodes with reference to timing and magnitude of ozone values. Model results show good potential for air quality prediction in the Mississippi Gulf coast within reasonable error limits of 10%. The emission inputs in the model need to be examined with sensitivity experiments using different available datasets to address this issue further. It is also proposed to conduct further simulations to study the impact of different spin up times on the model chemical species. This study brings out the importance of the prediction of meteorological variables, temperature, humidity and wind flow characteristics, in the daytime evolution of surface ozone apart from the precursor pollutants such as NO_2. Of the three PBL schemes, YSU stands superior to MYJ and ACM schemes and of the land surface physics schemes, SOIL and NOAH schemes produced better simulations both for meteorological fields and chemical species. Between NOAH and SOIL schemes, NOAH scheme is better taking into consideration of error metrics for all variables. The results are confirmative as YSU PBL and NOAH land surface schemes produced better simulation of both the meteorological fields and the chemical species of NO_2 and ozone in contrast to some earlier studies which have indicated YSU PBL scheme to be better for meteorological variables and MYJ scheme for ozone.

Acknowledgements

Authors thank for the support of the Atmospheric Dispersion Project (ADP) funded by U.S. Department of Commerce through National Oceanic and Atmospheric Administration (Silver Springs, MD); Contract #NA08 NWS4680056. The WRF/Chem model code is obtained from NCAR. The air data are obtained from EPA AIRS. Authors express sincere thanks to the anonymous reviewers for many helpful suggestions towards improvement of the manuscript.

References

Borge, R., Alexandrov, V., Del Vas, J.J., Lumbreras, J., Rodriguez, E., 2008. A comprehensive sensitivity analysis of the WRF model for air quality applications over the Iberian Peninsula. *Atmospheric Environment* 42, 8560-8574.

Byun, D.W., Ching, J.K.S., 1999. Science algorithms of the EPA Models-3 Community Multiscale Air Quality Model (CMAQ) Modeling System. EPA/600/R-99/030, US Environmental Protection Agency, Office of Research and Development, Washington, DC.

Challa, V.S., Indracanti, J., Rabarison, M.K., Patrick, C., Baham, J.M., Young, J., Hughes, R., Hardy, M.G., Swanier, S.J., Yerramilli, A., 2009. A simulation study of mesoscale coastal circulations in Mississippi gulf coast. *Atmospheric Research* 91, 9-25.

Challa, V.S., Indrcanti, J., Baham, J.M., Patrick, C., Rabarison, M.K., Young, J.H., Hughes, R., Swanier, S.J., Hardy, M.G., Yerramilli, A., 2008. Sensitivity of atmospheric dispersion simulations by HYSPLIT to the meteorological predictions from a meso-scale model. *Environmental Fluid Mechanics* 8, 367-387.

Chang, J. S., Middleton, P.B.., Stockwell, W.R., Binkowski, F.S., Byun, D.1989. The Regional Acid Deposition Model and Engineering Model, State-of-Science/Technology, Report 4, National Acid Precipitation Assessment Program, Washington, DC.

Chen, F., Dudhia, J. 2001. Coupling an advanced land surface-hydrology model with the Penn State-NCAR MM5 modeling system. Part I: model implementation and sensitivity. *Monthly Weather Review* 129, 569–585.

Cheng, W.Y.Y., Steenburgh, W.J., 2005. Evaluation of surface sensible weather forecasts by the WRF and the ETA models over the Western United States. *Weather and Forecasting* 20, 812-821.

Dudhia, J., 1996: A multi-layer soil temperature model for MM5. Preprints, *The Sixth PSU/NCAR Mesoscale Model Users' Workshop,* 22-24 July 1996, Boulder, Colorado, 49-50.

Chou, M.D., Suarez, M.J. 1994. An Efficient Thermal Infrared Radiation Parameterization For Use In General Circulation Models, Laboratory for Atmospheres, NASA Goddard Space Flight Center, Greenbelt, MDNASA Technical Memorandum, pp 85.

De Foy, B., Fast, J.D., Paech, S.J., Phillips, D., Walters, J.T., Coulter, R.L., Martin, T.J., Pekour, M.S., Shaw, W.J., Kastendeuch, P.P., Marley, N.A., Retama, A., Molina, L.T. 2008. Basin-scale wind transport during the MILAGRO field campaign and comparison to climatology using cluster analysis. *Atmospheric Chemistry and Physics* 8, 1209–1224.

De Foy, B., Varela, J.R., Molina, L.T., Molina, M.J., 2006. Rapid ventilation of the Mexico City basin and regional fate of the urban plume. *Atmospheric Chemistry and Physics* 6, 2321-2335.

Douglas, S.G., Haney, J.L., Wei, Y., Wang, B., Beckmann, S., 2005. Gulf Coast Ozone Study (GCOS) Modeling Analysis. Phase III: Additional future-year assessments. Prepared for the Southeast States Air Resources Managers (SESARM) and the Gulf Coast Ozone Study Operations Committee, by ICF International, San Rafael, CA (05-025). 245 pp.

Fast, J.D., Gustafson, W.I., Easter, R.C., Zaveri, R.A., Barnard, J.C., Chapman, E.G., Grell, G.A., Peckham, S.E., 2006. Evolution of ozone, particulates, and aerosol direct radiative forcing in the vicinity of Houston using a fully coupled meteorology chemistry aerosol model. *Journal of Geophysical Research-Atmospheres* 111, art. no. D21305.

Fast, J.D., Zhong, S.Y., 1998. Meteorological factors associated with inhomogeneous ozone concentrations within the Mexico City basin. *Journal of Geophysical Research-Atmospheres* 103, 18927-18946.

Giorgi, F., Meleux, F., 2007. Modelling the regional effects of climate change on air quality. *Comptes Rendus Geoscience* 339, 721-733.

Goncalves, M., Jimenez-Guerrero, P., Baldasano, J.M., 2009. Contribution of atmospheric processes affecting the dynamics of air pollution in south-western Europe during a typical summertime photochemical episode. *Atmospheric Chemistry and Physics* 9, 849-864.

Grell, G.A., Peckham, S.E., Schmitz, R., McKeen, S.A., Frost, G., Skamarock, W.C., Eder, B., 2005. Fully coupled "online" chemistry within the WRF model. *Atmospheric Environment* 39, 6957-6975.

Grell, G.A., 1993. Prognostic evaluation of assumptions used by cumulus parameterizations. *Monthly Weather Review* 121, 764-787.

Guenther, A., Zimmerman, P., Wildermuth, M., 1994. Natural volatile organic-compound emission rate estimates for united-states woodland landscapes. *Atmospheric Environment* 28, 1197-1210.

Guenther, A.B., Zimmerman, P.R., Harley, P.C., Monson, R.K., Fall, R., 1993. Isoprene and monoterpene emission rate variability - model evaluations and sensitivity analyses. *Journal of Geophysical Research-Atmospheres* 98, 12609-12617.

Hanna, S.R., 1994. Mesoscale meteorological model evaluation techniques with emphasis on needs of air quality models. *Meteorological Monographs* 25, 47-58.

Hong, S.Y., Noh, Y., Dudhia, J., 2006. A new vertical diffusion package with an explicit treatment of entrainment processes. *Monthly Weather Review* 134, 2318-2341.

Hu, X.M., Nielsen-Gammon, J.W., Zhang, F.Q., 2010. Evaluation of three planetary boundary layer schemes in the WRF model. *Journal of Applied Meteorology and Climatology* 49, 1831-1844.

Hurley, P.J., Manins, P.C., 1995. Meteorological modeling on high-ozone days in Perth, Western-Australia. *Journal of Applied Meteorology* 34, 1643-1652.

Janjic, Z. I. 2001. Nonsingular Implementation of the Mellor–Yamada Level 2.5 Scheme in the NCEP Meso Model. National Centers for Environmental Prediction Office, Note #437.

Janjic, Z.I., 1996. The surface layer in the NCEP Eta model, in Proceedings of the 11th Conference on Numerical Weather Prediction, American Meteorological Society, Norfolk, Va, USA, August 1996, pp 354–355.

Janjic, Z.I., 1990. The step-mountain coordinate - physical package. *Monthly Weather Review* 118, 1429-1443.

Jiang, F., Wang, T.J., Wang, T.T., Xie, M., Zhao, H., 2008. Numerical modeling of a continuous photochemical pollution episode in Hong Kong using WRF-CHEM. *Atmospheric Environment* 42, 8717-8727.

Jimenez, P., Jorba, O., Parra, R., Baldasano, J.M., 2006. Evaluation of MM5-EMICAT2000-CMAQ performance and sensitivity in complex terrain: High-resolution application to the northeastern Iberian Peninsula. *Atmospheric Environment* 40, 5056-5072.

Kleinman, L.I., Daum, P.H., Lee, Y.N., Nunnermacker, L.J., Springston, S.R., Weinstein-Lloyd, J., Hyde, P., Doskey, P., Rudolph, J., Fast, J., Berkowitz, C., 2003. Photochemical age determinations in the Phoenix Metropolitan area. *Journal of Geophysical Research-Atmospheres* 108, art. no. 4096.

Kleinman, L.I., Daum, P.H., Imre, D.G., Lee, J.H., Lee, Y.N., Nunnermacker, L.J., Springston, S.R., Weinstein-Lloyd, J., Newman, L., 2000. Ozone production in the New York City urban plume. *Journal of Geophysical Research-Atmospheres* 105, 14495-14511.

Lin, Y.L., Farley, R.D., Orville, H.D., 1983. Bulk parameterization of the snow field in a cloud model. *Journal of Climate and Applied Meteorology* 22, 1065-1092.

Madronich, S., 1987. Photodissociation in the atmosphere. 1. Actinic flux and the effects of ground reflections and clouds. *Journal of Geophysical Research-Atmospheres* 92, 9740-9752.

Mao, Q., Gautney, L.L., Cook, T.M., Jacobs, M.E., Smith, S.N., Kelsoe, J.J., 2006. Numerical experiments on MM5-CMAQ sensitivity to various PBL schemes. *Atmospheric Environment* 40, 3092-3110.

Misenis, C., Hu, X.M., Krishnan, S., Zhang, Y., Fast, J.D, 2006. Sensitivity of WRF/Chem predictions to meteorological schemes, *Proceedings of the 86th Annual AMS Annual Meeting, 14th Joint Conference on the Applications of Air Pollution Meteorology with the Air and Waste Management Associated*, 27 January–3 February, Atlanta, GA.

Mlawer, E.J., Taubman, S.J., Brown, P.D., Iacono, M.J., Clough, S.A., 1997. Radiative transfer for inhomogeneous atmosphere: RRTM, a validated correlated-k model for the longwave. *Journal of Geophysical Research* 102, 16663-16682.

Otte, T.L., 2008. The impact of nudging in the meteorological model for retrospective air quality simulations. Part I: Evaluation against national observation networks. *Journal of Applied Meteorology and Climatology* 47, 1853-1867.

Pleim, J.E., 2007a. A combined local and nonlocal closure model for the atmospheric boundary layer. Part I: Model description and testing. *Journal of Applied Meteorology and Climatology* 46, 1383-1395.

Pleim, J.E., 2007b. A combined local and nonlocal closure model for the atmospheric boundary layer. Part II: Application and evaluation in a mesoscale meteorological model. *Journal of Applied Meteorology and Climatology* 46, 1396-1409.

Pleim, J.E., Xiu, A., 1995. Development and testing of a surface flux and planetary boundary-layer model for application in mesoscale models. *Journal of Applied Meteorology* 34, 16-32.

Roux, G, Liu, Y, Monache, L.D, Sheu, R.Y, Warner, T.T., 2009. Verification of high resolution WRF-RTFDDA surface forecasts over mountains and plains. *10th WRF Users Workshop*, June 23 - 26, Boulder, Colorado, USA.

Shafran, P.C., Seaman, N.L., Gayno, G.A., 2000. Evaluation of numerical predictions of boundary layer structure during the Lake Michigan ozone study. *Journal of Applied Meteorology* 39, 412-426.

Simpson, D., Olendrzynacuteski, K., Semb, A., Storen, E., Unger, S., 1997. Photochemical Oxidant Modelling In Europe: Multi-annual Modelling and Source Receptor Relationships, EMEP MSC-W Report 3/97, Norwegian Meteorological Institute, Oslo, Norway.

Sistla, G., Zhou, N., Hao, W., Ku, J.Y., Rao, S.T., Bornstein, R., Freedman, F., Thunis, P., 1996. Effects of uncertainties in meteorological inputs on urban airshed model predictions and ozone control strategies. *Atmospheric Environment* 30, 2011-2025.

Skamarock, W.C., Klemp, J.B., Dudhia, J., Gill, D.O., Barker, D.M., Duda, M.G., Huang, X.Y., Wang, W., Powers, J.G., 2008. A Description of the Advanced Research WRF Version 3. NCAR Technical Note, NCAR/TN-475+STR. Mesoscale and Microscale Meteorology Division, National Center for Atmospheric Research, Boulder, Colorado, USA

Smirnova, T.G., Brown, J.M., Benjamin, S.G., Kim, D., 2000. Parameterization of cold-season processes in the maps land-surface scheme. *Journal of Geophysical Research-Atmospheres* 105, 4077-4086.

Stockwell, W.R., Middleton, P., Chang, J.S., 1990. The second generation regional acid deposition model chemical mechanism for regional air quality modeling. *Journal of Geophysical Research*, 95, 16343–16367.

Thielmann, A., Prevot, A.S.H., Staehelin, J., 2002. Sensitivity of ozone production derived from field measurements in the Italian Po basin. *Journal of Geophysical Research-Atmospheres* 107, 8194-8203.

Tie, X., Madronich, S., Li, G., Ying, Z., Weinheimer, A., Apel, E., Campos, T., 2009. Simulation of Mexico City plumes during the MIRAGE-Mex field campaign using the WRF-Chem model. *Atmospheric Chemistry and Physics* 9, 4621-4638.

West, J.J., Zavala, M.A., Molina, L.T., Molina, M.J., San Martini, F., McRae, G.J., Sosa-Iglesias, G., Arriaga-Colina, J.L., 2004. Modeling ozone photochemistry and evaluation of hydrocarbon emissions in the Mexico City metropolitan area. *Journal of Geophysical Research-Atmospheres* 109, art. no. D19312.

Willmott, C.J., 1982. Some comments on the evaluation of model performance. *Bulletin of the American Meteorological Society* 63, 1309-1313.

Yerramilli, A., Challa, S.V., Dodla, V.B.R., Dasari, H.P., Young, J.H, Patrick, C., Baham, J.M., Hughes, R., Hardy, M.G., Swanier, S.J., 2010. Simulation of surface ozone pollution in the Central Gulf Coast Region using WRF/Chem model: sensitivity to PBL and land surface physics. *Advances in Meteorology* 2010, art. no. 319138.

Yerramilli, A., Challa, S.V., Indracanti, J., Dasari, H., Baham,J., Patrick,C., Young, J., Hughes,R., White, L.D., Hardy, M.G., Swanier, S., 2008. Some observational and modeling studies of the atmospheric boundary layer at Mississippi Gulf coast for air pollution dispersion assessment. *International Journal of Environmental Research and Public Health* 5, 484-497.

Zaveri, R.A., Berkowitz, C.M., Kleinman, L.I., Springston, S.R., Doskey, P.V., Lonneman, W.A., Spicer, C.W., 2003. Ozone production efficiency and NO_x depletion in an urban plume: Interpretation of field observations and implications for evaluating O_3-NO_x-VOC sensitivity. *Journal of Geophysical Research-Atmospheres* 108, art. no. 4436.

Zhang, Y., Dubey, M.K., Olsen, S.C., Zheng, J., Zhang, R., 2009. Comparisons of WRF/Chem simulations in Mexico City with ground-based RAMA measurements during the 2006-MILAGRO. *Atmospheric Chemistry and Physics* 9, 3777-3798.

Zhang, Y., Liu, P., Pun, B., Seigneur, C., 2006. A comprehensive performance evaluation of MM5-CMAQ for the summer 1999 southern oxidants study episode - Part I: Evaluation protocols, databases, and meteorological predictions. *Atmospheric Environment* 40, 4825-4838.

Zhang, Y., Hu, X.M., Howell,G,W., Sills, E., Fast, J.D., Gustafson, W.I., Zaveri, R,A., Grell, G,A., Peckham, S,E., McKeen, S.A., 2005. Modeling Atmospheric Aerosols in WRF/CHEM. *WRF/MM5 Users' Workshop*, National Center for Atmospheric Research, June 2005, Boulder, USA.